

University of Kentucky

UKnowledge

University of Kentucky Master's Theses

Graduate School

2010

PASSIVE ATTITUDE STABILIZATION FOR SMALL SATELLITES

Samir Ahmed Rawashdeh

University of Kentucky, SAMIR.RAWASHDEH@GMAIL.COM

[Right click to open a feedback form in a new tab to let us know how this document benefits you.](#)

Recommended Citation

Rawashdeh, Samir Ahmed, "PASSIVE ATTITUDE STABILIZATION FOR SMALL SATELLITES" (2010).
University of Kentucky Master's Theses. 624.
https://uknowledge.uky.edu/gradschool_theses/624

This Thesis is brought to you for free and open access by the Graduate School at UKnowledge. It has been accepted for inclusion in University of Kentucky Master's Theses by an authorized administrator of UKnowledge. For more information, please contact UKnowledge@lsv.uky.edu.

ABSTRACT OF THESIS

PASSIVE ATTITUDE STABILIZATION FOR SMALL SATELLITES

This thesis addresses the problem of designing and evaluating passive satellite attitude control systems for small satellites. Passive stabilization techniques such as Gravity Gradient stabilization, Passive Magnetic Stabilization, and Aerodynamic stabilization in Low Earth Orbit utilize the geometric and magnetic design of a satellite and the orbit properties to passively provide attitude stabilization and basic pointing. The design of such stabilization systems can be done using a high fidelity simulation of the satellite and the environmental effects in the orbit under consideration to study the on-orbit behavior and the effectiveness of the stability system in overcoming the disturbance torques. The Orbit Propagator described in this thesis is developed to include models for orbit parameters, Gravity Gradient torque, Aerodynamic Torque, Magnetic Torque, and Magnetic Hysteresis Material for angular rate damping. Aerodynamic stabilization of a three-unit CubeSat with deployable side panels in a “shuttlecock” design is studied in detail. Finally, the Passive Magnetic Stabilization system of KySat-1, a one-unit CubeSat, is also described in detail and the simulation results are shown.

KEYWORDS: CubeSat, ADCS, Aerodynamic Satellite Stabilization, Passive Magnetic Stabilization

Samir Rawashdeh

December 3rd, 2009

PASSIVE ATTITUDE STABILIZATION FOR SMALL SATELLITES

By

Samir Ahmed Rawashdeh

James E. Lumpp, Jr.

Director of Thesis

Stephen D. Gedney

Director of Graduate Studies

December 3rd, 2009

RULES FOR THE USE OF THESES

Unpublished theses submitted for the Master's degree and deposited in the University of Kentucky Library are as a rule open for inspection, but are to be used only with due regard to the rights of the authors. Bibliographical references may be noted, but quotations or summaries of parts may be published only with the permission of the author, and with the usual scholarly acknowledgments.

Extensive copying or publication of the thesis in whole or in part also requires the consent of the Dean of the Graduate School of the University of Kentucky.

A library that borrows this thesis for use by its patrons is expected to secure the signature of each user.

Name

Date

THESIS

Samir Ahmed Rawashdeh

The Graduate School
University of Kentucky
2009

PASSIVE ATTITUDE STABILIZATION TECHNIQUES FOR SMALL SATELLITES

THESIS

A thesis submitted in partial fulfillment of the
requirements for the degree of Master of Science in Electrical Engineering in the
College of Engineering at the University of Kentucky

By

Samir Ahmed Rawashdeh

Haapavesi, Finland

Director: Dr. James E. Lumpp, Jr.,

Associate Professor of Electrical and Computer Engineering

Lexington, Kentucky

2009

Copyright © Samir Ahmed Rawashdeh 2009

To my beloved parents

ACKNOWLEDGEMENTS

I would like to begin by acknowledging my thesis advisor Dr. James E. Lumpp, Jr., for his support and guidance throughout the work in this thesis and in the projects and missions I had the opportunity to work on. I appreciate and greatly value the interest he has in my education and personal development. Special thanks also go to the colleagues and friends at the Space Systems Laboratory whose input I found essential in developing this work.

I must thank my parents for being an endless source of inspiration and motivation. My appreciation cannot be put in words, I cannot imagine coming this far without their support and vision. I would like to thank my brothers and sister and their families for being live examples for me to aspire to be like, and for always being supportive in so many ways throughout my journey.

Finally, I thank the advisors and all the people behind the Kentucky Space program for the opportunity to reach out to Space!

TABLE OF CONTENTS

| | |
|------------------------------------------------------|------------|
| ACKNOWLEDGEMENTS | iii |
| LIST OF TABLES | vi |
| LIST OF FIGURES | vii |
| 1 INTRODUCTION..... | 1 |
| 1.1 KENTUCKY SPACE ENTERPRISE | 1 |
| 1.2 CUBESAT NANO-SATELLITE STANDARD | 2 |
| 1.3 PROBLEM STATEMENT..... | 3 |
| 2 BACKGROUND..... | 5 |
| 2.1 REFERENCE FRAMES..... | 5 |
| 2.2 ASTRODYNAMICS | 7 |
| 2.2.1 Direction Cosine Matrix and Euler Angles..... | 8 |
| 2.2.2 Eigen Axis rotations..... | 9 |
| 2.2.3 Euler Symmetric Parameters (Quaternions) | 10 |
| 2.2.4 Kinematic Equations | 10 |
| 2.2.5 Dynamic Equation | 11 |
| 2.3 RELATED WORK ON PASSIVE STABILIZATION | 11 |
| 2.3.1 Gravity Gradient Stabilization | 12 |
| 2.3.2 Aerodynamic Stabilization..... | 12 |
| 2.3.3 Passive Magnetic Stabilization | 13 |
| 2.4 SIMULINK® MODEL BASED DESIGN..... | 15 |
| 3 ATTITUDE PROPAGATION | 17 |
| 3.1 ORBITAL DYNAMICS..... | 19 |
| 3.1.1 Gravitational Pull..... | 20 |
| 3.1.2 Keplerian Elements..... | 21 |
| 3.2 TORQUE MODELS | 22 |
| 3.2.1 Aerodynamic Drag..... | 22 |
| 3.2.1.1 Aerodynamic Geometric Representation..... | 24 |
| 3.2.1.2 Aerodynamic Torque Modeling | 25 |
| 3.2.1 Gravity Gradient | 27 |

| | |
|---------------------------------------------------------------|-----------|
| 3.2.1.1 Gravity Gradient Modeling | 28 |
| 3.2.1.2 Gravity Gradient Stabilization..... | 29 |
| 3.2.2 Magnetic Torques | 30 |
| 3.2.2.1 Magnetic Field Dipole Model..... | 32 |
| 3.2.2.2 Magnetic Torque Model | 33 |
| 3.2.3 Magnetic Hysteresis Material Angular Rate Damping | 34 |
| 3.2.4 Magnetic Hysteresis Modeling | 35 |
| 4 AEROSTABILIZED CUBESAT DESIGN..... | 39 |
| 4.1 DESIGN CONCEPT | 39 |
| 4.2 DESIGN SPACE ANALYSIS IN 1-DOF..... | 40 |
| 4.3 SIMULATION RESULTS | 46 |
| 5 PASSIVE MAGNETIC STABILIZATION | 48 |
| 5.1 INTRODUCTION | 48 |
| 5.2 DESIGN | 49 |
| 5.2.1 Magnets..... | 49 |
| 5.2.2 Hysteresis Damping | 51 |
| 5.3 SYSTEM PERFORMANCE..... | 54 |
| 6 CONCLUSIONS..... | 56 |
| 7 REFERENCES | 58 |
| VITA..... | 60 |

LIST OF TABLES

| | |
|-----------------------------------------------------------------------------------------|----|
| TABLE 2-1: SUMMARY OF ATTITUDE REPRESENTATIONS | 8 |
| TABLE 2-2: LIST OF SIMULINK SOLVERS..... | 16 |
| TABLE 4-1: AEROSTABILIZATION SIMULATION PARAMETERS | 46 |
| TABLE 5-1: WORST-CASE EXPECTED DISTURBANCE TORQUES FOR A 1-U CUBESAT AT 700 KM..... | 49 |
| TABLE 5-2: KYSAT-1 PASSIVE MAGNETIC STABILIZATION SYSTEM SUMMARY | 50 |
| TABLE 5-3: KYSAT-1 PASSIVE MAGNETIC STABILIZATION SYSTEM SIMULATION PARAMETERS | 54 |

LIST OF FIGURES

| | |
|--------------------------------------------------------------------------------------------------------------------------------------------------------------------------------------------|----|
| FIGURE 1-1: KYSAT-1 IS A 1-U CUBESAT DESIGNED BY KENTUCKY SPACE [1]..... | 2 |
| FIGURE 2-1: ECEF AND ECI REFERENCE FRAMES..... | 6 |
| FIGURE 3-1: ORBITAL ENVIRONMENT SIMULATOR | 18 |
| FIGURE 3-2: TRANSLATION DYNAMICS..... | 19 |
| FIGURE 3-3: SIMULINK® MODEL OF GRAVITATIONAL FORCE MODEL FOR AN ORBITING SATELLITE..... | 21 |
| FIGURE 3-4: NORAD TWO LINE ELEMENTS..... | 22 |
| FIGURE 3-5: GEOMETRY REPRESENTATION FOR AERODYNAMIC TORQUE PROFILING | 24 |
| FIGURE 3-6: SIMULINK® MODEL OF AERODYNAMIC TORQUE..... | 26 |
| FIGURE 3-7: SIMULINK® MODEL OF GRAVITY GRADIENT TORQUE..... | 28 |
| FIGURE 3-8: SIMULINK® MODEL OF L-SHELL MAGNETIC MODEL | 33 |
| FIGURE 3-9: SIMULINK® MODEL OF MAGNETIC TORQUE DUE TO PERMANENT MAGNETS | 34 |
| FIGURE 3-10: HYSTERESIS LOOP MODELING IN SIMULINK® [9] | 37 |
| FIGURE 3-11: SIMULINK® MODEL OF MAGNETIC TORQUE DUE TO HYSTERESIS MATERIAL | 37 |
| FIGURE 4-1: AERODYNAMICALLY STABLE CUBESAT DESIGN CONCEPT | 40 |
| FIGURE 4-2: GEOMETRY OF SATELLITE DESIGN..... | 41 |
| FIGURE 4-3: PITCH TORQUE PROFILES SHOWING TORQUE EXPERIENCED AS A FUNCTION OF THE ANGLE TO VELOCITY VECTOR (Φ) | 42 |
| FIGURE 4-4: AERODYNAMIC STIFFNESS AT 400 KM ALTITUDE FOR A RANGE OF PANEL LENGTHS (Λ)..... | 43 |
| FIGURE 4-5: CONSTANT STIFFNESS CURVES AT 400KM ALTITUDE. PANEL LENGTH (Λ) AND DEPLOYMENT ANGLE (Θ) COMBINATIONS TO OBTAIN EQUAL STEADY-STATE PERFORMANCE. | 45 |
| FIGURE 4-6: EFFECT OF VARYING THE PANEL LENGTH (Λ) AT DIFFERENT ALTITUDES FOR PANELS DEPLOYED AT $\Theta = 50$ DEG, COMPUTED USING ACTUAL CALCULATED TORQUE PROFILES. | 45 |
| FIGURE 4-7: SIMULATED TIME RESPONSE OF AEROSTABILIZED SATELLITE WITH 20CM | |

| | |
|--------------------------------------------------------------------------------------------------------------------------------|----|
| PANELS DEPLOYED AT 30 DEGREES, AT 350 KM. | 47 |
| FIGURE 5-1: KYSAT-1, PASSIVE MAGNETIC STABILIZATION SYSTEM IS USED FOR ANTENNA ORIENTATION AND COARSE CAMERA POINTING. | 48 |
| FIGURE 5-2: KYSAT-1 FOUR PERMANENT MAGNET SETS..... | 50 |
| FIGURE 5-3: ONE OF FOUR ALINCO-5 PERMANENT MAGNET SETS ON BOARD KYSAT-1. .. | 51 |
| FIGURE 5-4: HYSTERESIS MATERIAL AMOUNT DESIGN PLOTS..... | 53 |
| FIGURE 5-5: HYSTERESIS STRIPS ON THE BACK OF A SOLAR BOARD, ON KYSAT-1 | 54 |
| FIGURE 5-6: KYSAT-1 RESPONSE PLOT | 55 |

1 Introduction

This chapter introduces the Kentucky Space program, the CubeSat standard, and the problem of analyzing the performance of passive attitude stabilization systems. Chapter 2 introduces basic astrodynamics, the coordinate systems and attitude representations used in the implementation of the simulation environment, and a survey of related work on passive stabilization of small satellites. Chapter 3 develops the Attitude Propagator that includes Orbit Parameters, Gravity Gradient torque, Aerodynamic Torque, Magnetic Torque, and Magnetic Hysteresis Material. Chapter 4 discusses the aerodynamic stabilization of a three-unit CubeSat with deployable side panels in a “shuttlecock” design. Finally, chapter 5 discusses the Passive Magnetic Stabilization system of KySat-1, a one-unit CubeSat.

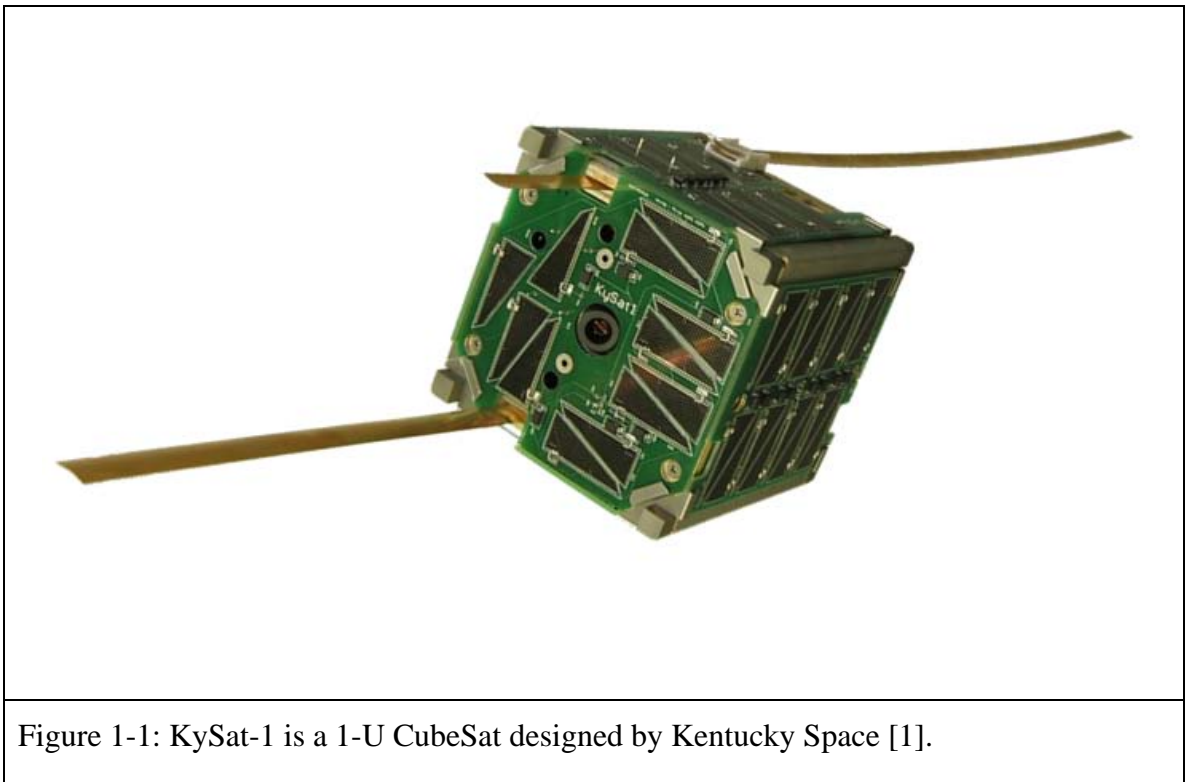
1.1 Kentucky Space Enterprise

The Kentucky Space Enterprise began as a partnership between several universities and industry partners in the state of Kentucky. The initial goal was to develop, launch, and operate a CubeSat within the state of Kentucky. Sub-orbital and High altitude balloon missions with shorter durations were introduced within the program to train new students on development processes, test and qualify hardware in low risk missions, and gather data on space and near-space environments.

KySat-1, the first satellite project by Kentucky Space, is a 1-U CubeSat scheduled to launch in 2010 on a NASA mission. It is stabilized using a set of permanent magnets and a certain amount of hysteresis material. Passive Magnetic Stabilization aligns one axis of a satellite with the earth’s magnetic field in orbit. In a polar orbit, KySat-1 should perform two rotations per orbit. The design was such that the main VHF and UHF communication antennas would face the ground stations antennas in a pass over Kentucky. Chapter 5 details the Passive Magnetic Stability of KySat-1.

1.2 CubeSat Nano-Satellite Standard

Small spacecraft technology has been shown to reduce cost and development time and to maximize science return. The CubeSat Standard (10x10x10 cm³ with mass ≤ 1 kg) was developed by Stanford University and California Polytechnic State University (CalPoly) as a means to standardize pico-satellite buses, structures, and subsystems [1]. The current CubeSat standard allows two or three cubes to be “stacked” to construct larger 2-U and 3-U CubeSats. CalPoly has also developed a standardized Launch Vehicle Interface (LVI) to accommodate CubeSats known as the Poly-Picosatellite Orbital Deployer (P-POD) which can launch up to 3-U’s in several configurations (one 3-U, three 1-U’s, etc). This system has opened space exploration to smaller organizations, in particular university student teams, that would not otherwise have the opportunity to build, launch, and operate spacecraft. Figure 1-1 is an example of a 1-U CubeSat.



The P-POD and the CubeSat Standard have enjoyed much success since the first CubeSat launch in 2003. The P-POD has flown on four different launch vehicles: the Rocket

operated by Eurockot, the Dnepr operated by ISC Kosmotras, the Minotaur from Orbital Sciences, and the Falcon-1 from SpaceX. Six P-PODs have been successfully deployed to date containing twelve CubeSats. There have also been several other international CubeSat launches utilizing other LVT's.

CubeSats are designed for high risk, low cost access to space; however, the small size of the CubeSat imposes substantial mass, volume, and power constraints. Therefore novel spacecraft designs can be investigated and are often necessary to meet the constraints of the standard. In particular, attitude control for CubeSats remains a fairly open problem. Experiments have been conducted using actuators such as reaction wheels, magnetic torque coils, and micro-thrusters. Active control actuators in general are very well understood and are widely used. The challenge remains to be the miniaturization of these actuators, especially momentum storage devices, to comply with the CubeSat form factor and to conform to the strict mass and power budgets. Passive methods such as passive magnetic stabilization, aerostabilization, and gravity gradient stabilization are robust, include no moving parts, require little to no power, and are an attractive option for several applications. The focus thus far within Kentucky Space has been on passive and robust stabilization techniques.

1.3 Problem Statement

Passive Satellite Stabilization using either Passive Permanent Magnets, a Gravity Gradient bias, or an aerodynamically stable design simplifies the implementation once a design has been put in place. However, the performance of a certain design is a function of its attitude dynamics under environmental torques which depend on the expected orbit, altitude, and the satellite geometry and mass properties. In order to design and quantify the performance of a certain satellite a high fidelity simulation of the satellite parameters (geometry, design, and orbit) and the environmental torques affecting it is required.

In the case of active control actuators such as reaction wheels, the design choice would be a function of the order of magnitude of the worst case expected torque on orbit, the

minimum required slew times, and desired pointing accuracy. A simulation to propagate the satellite in orbit may not be necessary, since the reaction wheels can be chosen to overcome the worst expected disturbance torques. Simpler simulations or calculations can be done on these special cases to quantify the drift and errors due to actuator resolution in order to quantify the pointing accuracy.

In passive techniques, however, stability is often achieved on only two of three rotation axes. Rotation around the magnet axis in magnetic stabilization is uncontrolled, as well as roll in aerodynamic stability and rotations about the gravity gradient boom axis. It is difficult to predict the behavior about these uncontrolled axes analytically. This motivates the development of a high fidelity simulation to propagate the attitude in 6DOF.

The major torques affecting small satellites in LEO are Gravity Gradient, Aerodynamic Drag, and torques induced by the Earth's Magnetic Field. Solar pressure is typically at least one order of magnitude smaller than any of the other torques since the surface area of CubeSats is typically small. One of these environmental effects can be utilized in the satellite design to be greater than the other environmental torques and provide stability. That concept is the essence of the passive stabilization techniques discussed in this thesis. The attitude propagator needs to include the major torque sources, the design of a stable system can be found by running simulations on a range of design variables and selecting a suitable value.

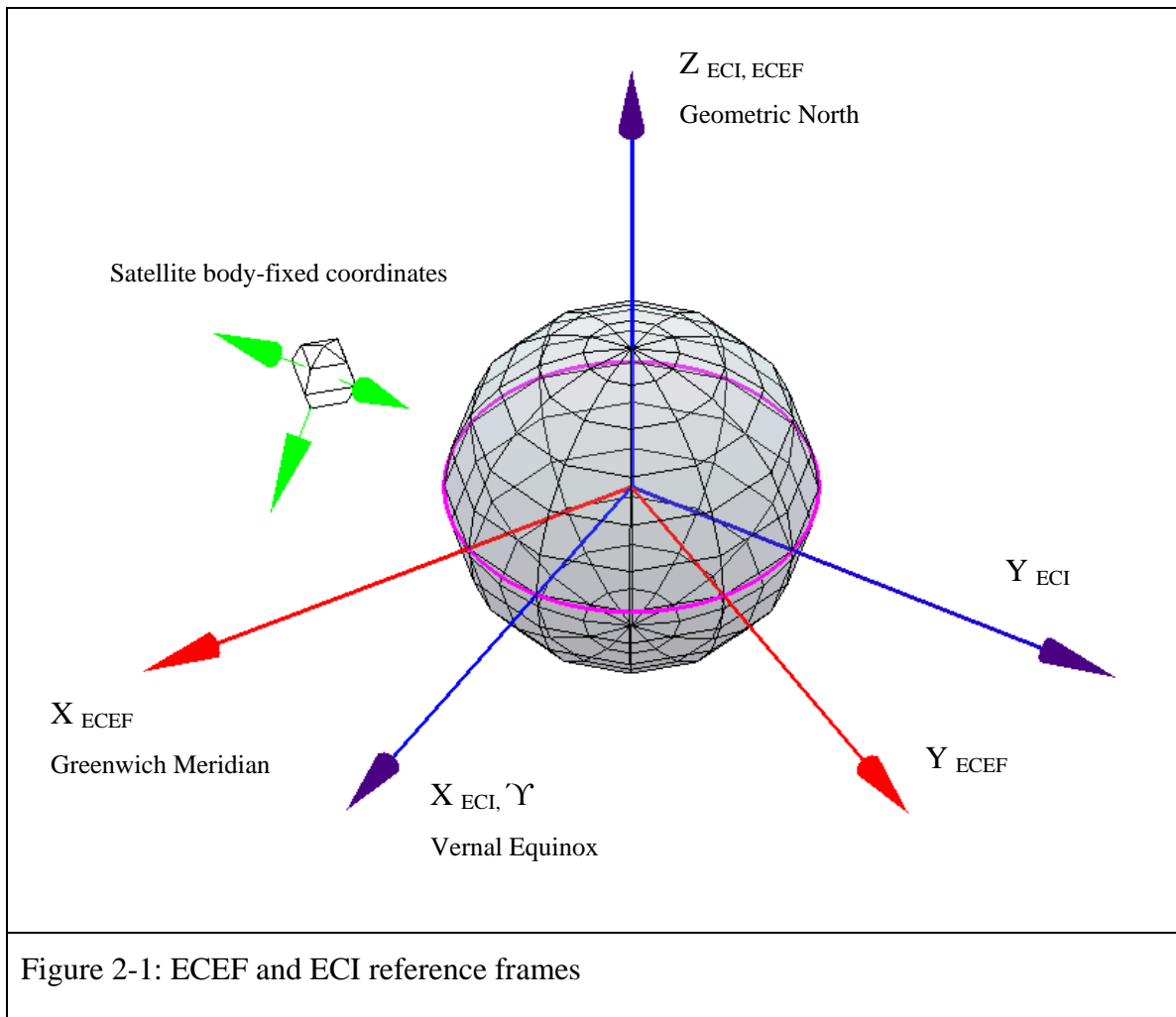
2 Background

2.1 Reference Frames

The three main reference frames that are used in this work are explained in this section. The Earth Centered Inertial frame is taken as the main reference to observe and study the Body-fixed frame (satellite attitude). The Earth Centered Earth Fixed reference frame is a body-fixed coordinate system centered in Earth, and rotates relative the Earth Centered Inertial frame.

Earth Centered Earth Fixed (ECEF). This reference frame is earth centered, having a z-axis that lines up with the earth spin axis pointing towards the celestial north pole. The x-axis extends to the zero latitude and longitude point, i.e. the intersection of the Equator and the prime meridian passing through Greenwich, UK. The y-axis is such that it completes the right hand rule. The ECEF frame is convenient to describe phenomena that are earth-fixed, such as ground stations, earth targets, and the geomagnetic field.

Earth Centered Inertial (ECI). This reference frame is earth centered, with the z-axis towards the celestial north Pole. The x-axis points towards the Vernal Equinox, which is the intersection of the ecliptic plane with the equatorial plane, at the ascending node. The y-axis completes the right hand rule.



The ECI frame is considered as the main reference frame. Satellite orbits are planar in ECI. The ECEF frame rotates once around ECI approximately every 24 hours. ECEF is convenient for earth referenced phenomena. For example, the translation from latitude and longitude to ECEF is a direct calculation independent of time, and the Earth's magnetic dipole is also fixed in ECEF and rotating with respect to ECI.

With the time of day factored into the transformations, the rotation between the ECI and ECEF frames can be calculated. These transformations are necessary in calculating the magnetic field at a certain position in orbit in ECI. The Magnetic Model is described in detail in section 3.2.2.1.

Finally, the Body-Fixed frame, as the name suggests, is defined by the satellite geometry by user convention. The rotation between the body-fixed frame and ECI is considered the attitude of the satellite, which is the focus in attitude control problems.

2.2 Astrodynamics

Astrodynamics is the study of the motion of man-made objects in space, subject to both natural and artificially induced forces [2]. The definition combines both Orbital Dynamics and Attitude Dynamics. Orbital Dynamics describe an object's translation through orbit under gravitational pull from Earth and other celestial objects, and changes in orbit due to spacecraft maneuvers or orbit decay from atmospheric drag. Attitude Dynamics pertain to the representation and dynamics of rotational changes of a satellite about its center of mass. There are numerous mathematical representations for satellite attitudes, each convenient for certain applications or control modes [3][4].

Orbit propagation, in contrast to Attitude Propagation, is concerned with the perturbations effects and satellite translation from an ideal orbit, such as orbit decay due to atmospheric drag. In a study of Attitude Dynamics, only knowledge of the position of the satellite in orbit is required to calculate most parameters, such as the magnetic field intensity or gravity vector, in turn to compute the angular moments affecting the satellite at that point. In addition, attitude maneuvers occur on a significantly smaller time scale compared to orbit variations, so the orbit is assumed constant over the simulation time (typically a few days, or tens of orbits). The analysis on the variations in orbit parameters with time has little effect on attitude dynamics and is beyond the scope of this work. The translational dynamics are simplified to the two-body equations with only Earth gravitational pull acting on the satellite. Section 3.1 on Orbit Dynamics details the considerations and implementation.

Euler rotation angles and Quaternion representations are used in this text to define attitude kinematics and dynamics. Table 2-1 summarizes commonly used mathematical models [3][4].

Table 2-1: Summary of Attitude Representations

| Parameterization | Advantages | Disadvantages |
|-------------------------|-------------------------------------------------------------------------------------------------------------------------------------------------------------------------------------------------------------|---------------------------------------------------------------------------------------------------------------------------------------------------------------------------------|
| Direction Cosine Matrix | <ul style="list-style-type: none"> -No singularities -No trigonometric Functions -Clear physical interpretation -Convenient product rule for successive rotations | <ul style="list-style-type: none"> -Six redundant parameters |
| Euler Angles | <ul style="list-style-type: none"> -No redundant parameters -Clear physical interpretation | <ul style="list-style-type: none"> -Singularities at some angles -Trigonometric functions -No convenient product rule for successive rotations |
| Eigen Axis | <ul style="list-style-type: none"> -Clear physical interpretation | <ul style="list-style-type: none"> -Axis undefined when rotation is 0° -Trigonometric Functions |
| Quaternions | <ul style="list-style-type: none"> -No singularities -No trigonometric functions -Convenient product rule for successive rotations | <ul style="list-style-type: none"> -One redundant parameter -No obvious physical interpretation |

2.2.1 Direction Cosine Matrix and Euler Angles

The Direction Cosine Matrix (DCM) is a 3 by 3 matrix that defines the rotations between two reference frames. Here the rotation matrix C_{ba} describes the rotation between frame a and frame b ; the vector x is rotated from a to b :

$$\vec{x}_b = C_{ba} \vec{x}_a$$

The rotation between two frames can be broken down into a sequence of rotations about the three body orthogonal axes such that:

$$C = R_1(\theta_1) R_2(\theta_2) R_3(\theta_3)$$

$$R_1(\theta_1) = \begin{bmatrix} 1 & 0 & 0 \\ 0 & \cos(\theta_1) & \sin(\theta_1) \\ 0 & -\sin(\theta_1) & \cos(\theta_1) \end{bmatrix}$$

$$R_2(\theta_2) = \begin{bmatrix} \cos(\theta_2) & 0 & -\sin(\theta_2) \\ 0 & 1 & 0 \\ \sin(\theta_2) & 0 & \cos(\theta_2) \end{bmatrix}$$

$$\mathbf{R}_3(\theta_3) = \begin{bmatrix} \cos(\theta_3) & \sin(\theta_3) & 0 \\ -\sin(\theta_3) & \cos(\theta_3) & 0 \\ 0 & 0 & 1 \end{bmatrix}$$

These rotation angles $\theta_1, \theta_2, \theta_3$ are referred to as Euler rotation angles. The order of the rotations matters and affects the definition of the satellite rotations. In this work, the rotations are chosen to be around the three orthogonal body axes; roll, pitch, and yaw. The angles $\theta_1, \theta_2, \theta_3$ represent rotations about those axes, respectively.

Euler rotation angles efficiently describe a rotation (or an objects orientation) with three parameters. However, dynamic equations suffer from singularities when described in Euler Angles, i.e. trigonometric functions appear in the denominator of some dynamic and kinematic equations which become undefined for certain values of rotation angles when a zero appears in the denominator. However, Euler angles are intuitive and frequently used outside the dynamic and kinematic equations.

The Direction Cosine Matrix (DCM) describes a rotation with 9 parameters, making it inefficient. It is also non-intuitive. However, vector rotations under this representation are simply a matrix multiplication by the DCM. When vector rotations are modeled, the rotation matrix (DCM) is found from the Euler angles or the Quaternion representation to perform the rotation using a matrix multiplication.

2.2.2 Eigen Axis rotations

The Eigen Axis representation of a rotation between two frames, defines the transformation as a single rotation about a complex Eigen-axis. The Eigen axis is the unique solution to the following equality for the rotation between the vectors a and b :

$$e_1 \vec{a}_1 + e_2 \vec{a}_2 + e_3 \vec{a}_3 = e_1 \vec{b}_1 + e_2 \vec{b}_2 + e_3 \vec{b}_3$$

$$\mathbf{e} = (e_1, e_2, e_3)^T$$

The Eigen-axis's orientation relative to both frames remains unchanged [4]. Intuitively, it can be thought of as the axis around which the object rotates to perform an attitude maneuver with a single rotation, as opposed to a sequence of rotations around the body

axes (Euler Angles). The rotation angle about the Eigen-axis can be calculated from:

$$\cos(\theta) = \frac{1}{2}(C_{11} + C_{22} + C_{33} - 1)$$

Where C_{11}, C_{22}, C_{33} are the diagonal elements in the Direction Cosine Matrix. The Eigen axis representation is not used in the formulation of concepts in this thesis. The brief concept is introduced here to develop the Quaternion representation that follows.

2.2.3 Euler Symmetric Parameters (Quaternions)

Quaternion elements do not carry a direct intuitive meaning. The Quaternion representation however simplifies the kinematic and dynamic equations and does not suffer from singularities which do occur in Euler angle representations.

The quaternion vector that defines the rotation between two frames is defined based on elements of the Eigen Axis rotations representation, as:

$$\begin{aligned} \mathbf{q} &= (q_1, q_2, q_3)^T = \mathbf{e} \sin\left(\frac{\theta}{2}\right) \\ q_1 &\stackrel{\text{def}}{=} e_1 \sin\left(\frac{\theta}{2}\right) \\ q_2 &\stackrel{\text{def}}{=} e_2 \sin\left(\frac{\theta}{2}\right) \\ q_3 &\stackrel{\text{def}}{=} e_3 \sin\left(\frac{\theta}{2}\right) \\ q_4 &\stackrel{\text{def}}{=} \cos\left(\frac{\theta}{2}\right) \end{aligned}$$

2.2.4 Kinematic Equations

The kinematic equations of torque free motion representing the effect of body angular rates on the attitude can be formulated as:

$$\dot{\mathbf{C}} + \mathbf{\Omega C} = 0$$

Where $\mathbf{\Omega}$ is defined with the body angular rotation rates as:

$$\mathbf{\Omega} = \begin{bmatrix} 0 & -\omega_3 & \omega_2 \\ \omega_3 & 0 & -\omega_1 \\ -\omega_2 & \omega_1 & 0 \end{bmatrix}$$

The same kinematic equation in Quaternion representation can be expressed as:

$$\begin{aligned} \dot{\mathbf{q}} &= \frac{1}{2} (q_4 \boldsymbol{\omega} - \boldsymbol{\omega} \times \mathbf{q}) \\ \dot{q}_4 &= -\frac{1}{2} \boldsymbol{\omega}^T \mathbf{q} \end{aligned}$$

2.2.5 Dynamic Equation

The dynamic equation in Quaternion representation, which is used in this thesis exclusively, describes the effect external angular moments have on the change in the body's angular rates:

$$\begin{aligned} J\dot{\boldsymbol{\omega}} + \boldsymbol{\omega} \times J\boldsymbol{\omega} &= \mathbf{M} \\ \mathbf{M} &= \begin{bmatrix} M_1 \\ M_2 \\ M_3 \end{bmatrix} \end{aligned}$$

Where J is the body's inertia matrix, and M is the external angular moment applied to the body's main axes. It is noted that the change (time derivative) in the angular rotation rates $\boldsymbol{\omega}$, is a function of the angular body rates and the inertia matrix. Gyroscopic stiffness of a spinning object being rigid to external torques is implicit in the dynamic equation. This is further motivation to implement a dynamic attitude propagator to study spin stabilized satellites in the future.

2.3 Related Work on Passive Stabilization

Passive attitude stabilization with no processing or power requirements have been demonstrated for small satellites. Related work on Gravity gradient, aerodynamic, and magnetic stability is discussed in this section. Several of these techniques have been developed for the CubeSat form factor, some of which were flight tested in orbit.

2.3.1 Gravity Gradient Stabilization

The gravity gradient phenomena can be used to stabilize satellites in a nadir pointing attitude. In orbit, the differences in the Earth's gravitational pull across the satellite mass due to the minor difference in the distance to earth becomes a significant source of torques. For cylindrically shaped satellites, the length of the satellite will tend to align with the nadir vector. The phenomenon and mathematical modeling are explained in more detail in the Attitude Propagator section 3.2.1. Gravity Gradient stabilization provides nadir-pointing stabilization acting in pitch and roll to maintain a nadir-pointing attitude while leaving yaw uncontrolled.

IceCube-1 and IceCube-2 were developed with gravity gradient booms, but were unfortunately lost in launch failures [5] preventing on-orbit verification. Several other CubeSats currently under development include deployable booms in their designs[6].

2.3.2 Aerodynamic Stabilization

The atmospheric density decreases exponentially with altitude. For LEO orbits around 500km, the atmosphere is sufficiently substantial to drag satellites causing increased orbit decay and angular moments. Aerodynamics can be used to provide stability aligning the satellite with the velocity vector. Aerodynamic stability typically acts in pitch and yaw to maintain a ram-facing attitude while leaving roll uncontrolled.

Aerostabilization in LEO was flight tested as an experiment on the shuttle Endeavour in 1996.4,5 The Passive Aerodynamically Stabilized Magnetically-damped Satellite (PAMS) experiment demonstrated the feasibility of aerostabilization with magnetic hysteresis material for damping. The PAMS satellite was designed as a cylindrical “stove pipe” having a significantly thicker shell on one end to shift the center of mass of the satellite and produce an aerodynamically stable design for altitudes from 250 to 325 km. The simulations were based on free-molecular aerodynamics and incorporated variations in atmospheric density, global winds, and solar radiation. It also simulated the behavior of hysteresis material cycling in a model of the earth's magnetic field, and showed

damping within 1 day, and a worst-case cone angle of 9 degrees.

The dimensions of PAMS are similar to those of CubeSats; however the CubeSat Standard does not allow such an offset in the center of mass unless a shift is performed post-deployment. In the design studied here, a “shuttlecock” design is used as an effective way to shift the center of drag pressure behind the center of mass after orbit insertion while still conforming to the CubeSat standard.

Psiaki [7] proposes a “shuttlecock” design to obtain aerodynamic stability. The system uses four deployable “feathers” that resemble retractable tape measures extending from a 1-U CubeSat. It also incorporates active magnetic torque coils for damping and was shown through simulation to achieve stability for all altitudes below 500 km. The design was evaluated by studying and comparing a simplified stiffness model with a model based on free-molecular aerodynamics. The narrow one-meter-long feathers were deployed at 12 degrees. The design was shown to stop tumbling within 1 hour, and achieved a steady-state pointing error of 2 degrees within 15 hours.

2.3.3 Passive Magnetic Stabilization

A set of permanent magnets on board spacecraft in LEO align the satellite with the Earth’s magnetic field lines it experiences in orbit. The attitude of a magnetically stabilized satellite is a function of the orbit and the magnetic field lines along the orbit. In a low inclination orbit, the magnets will tend to point towards the magnetic north like a compass needle, whereas in a higher inclination orbit such as polar orbit, a magnetically stabilized satellite would perform two cycles per orbit, where it would line up north-to-south over the equator, and tumble over the Earth’s magnetic poles to line up with the Earth’s magnetic dipole.

KySat-1 [1], a 1-U CubeSat by the Kentucky Space Consortium, utilizes Passive Magnetic Stabilization for attitude stabilization and antenna pointing. The design details on the attitude control of KySat-1 are developed in Chapter 5.

Passive Magnetic Stabilization is a popular technique to stabilize CubeSats and has been demonstrated in orbit. QuakeSat, Delfi-C3, and GeneSat are some of several CubeSats currently in orbit utilizing permanent magnets for stabilization.

Menges et al. [8] describe a study on the passive magnetic stabilization system of Spartnik, a micro-satellite by San Jose State University. A set of differential equations describing the equations of motion were solved for different scenarios. The analysis is mainly on the sensitivity of the simulation to variations in the inertia matrix, magnet strength, and spin rate about the magnet axis which is induced in Spartnik using “solar paddles”. Spin about the magnet axis, if present, introduces gyroscopic stiffness about the magnet axis. The design approach was to find design choices with comfortable margin for inaccuracies to guarantee successful operation in orbit, parameters that are a function of the orbital environment were set instead of simulated, and they were varied to study the sensitivity to those parameters. The effect of disturbance torques such as gravity gradient and aerodynamic effects were not simulated, nor was the magnetic hysteresis material which provided damping.

CubeSim [9] is a widely used open source tool to aid in the design of passive magnetic stabilized satellites. CubeSim is an orbit propagator developed in Simulink® that includes analysis tools for power generation and thermal issues. It also includes an Earth magnetic model and three hysteresis loop approximations to aid in calculating the required ration of hysteresis material to permanent magnets. However, the strength of the included magnets should be strong enough to overcome disturbance torques, which is not included in CubeSim. The preliminary design of KySat-1 was developed using CubeSim, and was later verified by the Orbital Environment Simulator developed in this thesis which included other disturbance and environmental effects beyond permanent magnets and hysteresis.

2.4 Simulink® Model Based Design

Simulink® is a MATLAB tool for graphical modeling and simulation. The Simulink® graphical environment is a convenient design and simulation tool for time-varying dynamic systems, and can be used to simulate embedded systems and develop on target Digital Signal Processors (DSP). Simulink® is mainly used in this work as a differential equation solver with a convenient interface and a library of tools to allow quick development.

Several differential equation solvers are available under Simulink with varying performance [10]. Several parameters for each solver, as well as error tolerance, are adjustable. The tradeoff is mostly between accuracy and simulation time. Simulink® divides solvers into fixed-step and variable step solvers. Variable-step solvers reduce the time step when model states are rapidly changing to increase accuracy, and lengthen the time step when changes in the system are slow to reduce unnecessary computations and reduce simulation time. Table 2-2: List of Simulink Solvers summarizes the solvers available under Simulink. More details can be found in the Simulink documentation [10].

In the development and debugging of the modules under this work, and to test preliminary results, variable-step solvers are used to produce quick results. For reported results, the same simulation is run across several solvers, to ensure accuracy. Further accuracy is achieved by reducing the tolerance to error and time step for the solvers. Simulations run significantly longer with these settings, however results are produced with higher confidence [10].

Table 2-2: List of Simulink Solvers

| Fixed Step Solvers | Description |
|------------------------------|---------------------------------------------------------------------------------------------------------------------------------------------------------------------------------------------|
| ode1 | Euler's Method |
| ode2 | Heun's Method |
| ode3 | Bogacki-Shampine Formula |
| ode4 | Fourth-Order Runge-Kutta (RK4) Formula |
| ode5 | Dormand-Prince Formula |
| Variable Step Solvers | Description |
| ode45 | Based on an explicit Runge-Kutta (4,5) formula, the Dormand-Prince pair. |
| ode23 | Also based on an explicit Runge-Kutta (2,3) pair of Bogacki and Shampine. |
| ode113 | A variable-order Adams-Bashforth-Moulton PECE solver. |
| ode15s | A variable-order solver based on the numerical differentiation formulas (NDFs). |
| ode23s | Based on a modified Rosenbrock formula of order two. |
| ode23t | An implementation of the trapezoidal rule using a "free" interpolant. |
| ode23tb | An implementation of TR-BDF2, an implicit Runge-Kutta formula with a first stage that is a trapezoidal rule step and a second stage that is a backward differentiation formula of order two |

3 Attitude Propagation

It is challenging to quantify the pointing accuracy of a control technique and its performance under disturbance torques without modeling and simulations. This is especially true for varying environments such as a satellite in orbit, where solar pressure has its effect for only part of the orbit, and the magnetic field observed by the satellite performs two cycles per orbit, and earth magnetic dipole performs a rotation every 24 hours. Resonances could occur on the order of these variances which may be unpredictable analytically.

This chapter describes the attitude propagator implemented in Simulink® that includes the orbital and attitude dynamics components. Position in orbit is initialized using Keplerian orbital elements and propagated using a two-body model. The satellite's attitude is propagated using models for aerodynamic effects, gravity gradient, and magnetic effects. The attitude propagator is used to observe and animate the satellite behavior under the expected forces and moments in orbit. It can be used to evaluate the performance of passive control technique. The chapters following the development of the attitude propagator highlight systems that employ an environmental effect to overcome the other effects and achieve stability. Chapter 4 highlights an aerodynamically stable design that resembles a shuttlecock. KySat-1 in chapter 5 uses permanent magnets to align itself with the magnetic field in a polar orbit.

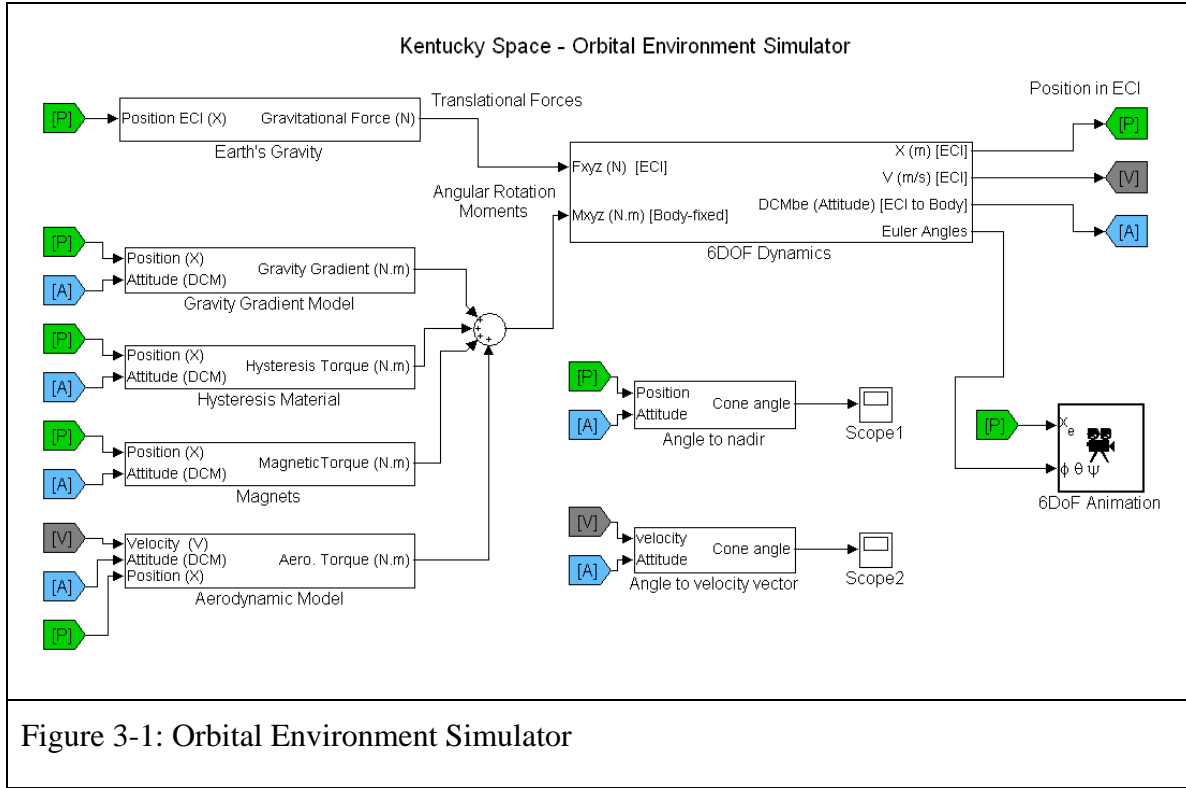


Figure 3-1: Orbital Environment Simulator

The Orbital Environment Simulator was developed to serve as a basis to help predict different scenarios and satellite configurations in orbit. Figure 3-1 shows the implementation in Simulink®. The satellite dynamics are defined in the 6-DOF block, which includes the quaternion implementation of the dynamics and kinematic equations described in section 2.2

$$J\dot{\omega} + \omega \times J\omega = M$$

And,

$$\dot{q} = \frac{1}{2}(q_4\omega - \omega \times q)$$

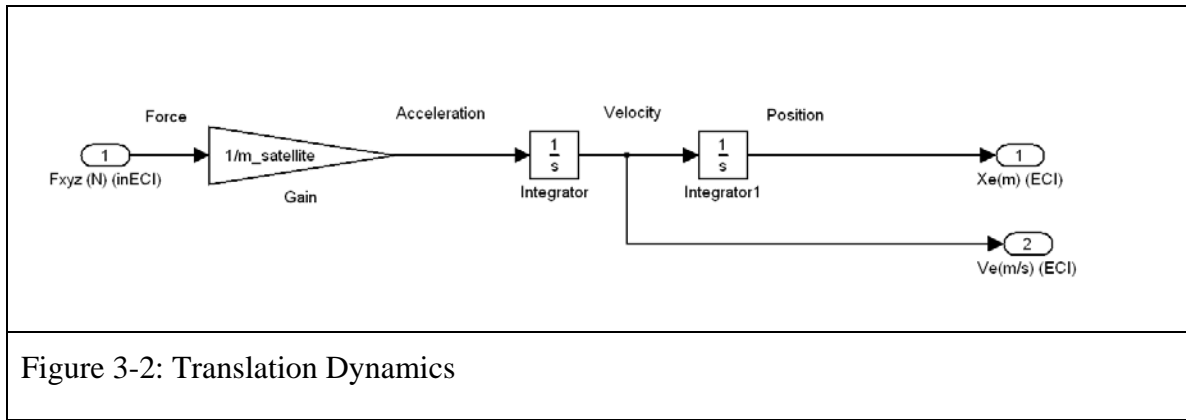
$$\dot{q}_4 = -\frac{1}{2}\omega^T q$$

The angular rotations in the 6-DOF Dynamics block are implemented using these equations in body-frame. Therefore, in the rest of the Orbital Environment Simulator, environmental torques that are calculated in other parts of the model must be rotated to body-frame and applied to the dynamics block.

Orbital dynamics are applied in the Earth-Centered Inertial (ECI) frame for simplification. The acceleration of the satellite towards earth is a function of the gravitational force and the mass of the satellite.

$$\ddot{\mathbf{X}} = \mathbf{F}_{gravity}/m_{satellite}$$

The velocity in orbit is the first integral of the equation, while the second integral results in the position of the satellite. Both the position and velocity are necessary to calculate several parameters and environmental effects, as discussed in the following sections highlighting the other modules in the model.



Some observation modules are also implemented to produce data to illustrate the calculated attitude. For ram-facing stability using aerodynamics the angle to the velocity vector is of interest, whereas for gravity-gradient stabilization the attitude relative to nadir is recorded. Finally, a module tracking the attitude relative to the Earth's magnetic field lines was implemented. The angle between two unit vector is calculated simply as:

$$\theta_{error} = \cos^{-1}(\mathbf{u}_1 \cdot \mathbf{u}_2)$$

3.1 Orbital Dynamics

The first element in the satellite attitude propagator is an orbit propagator. The Earth's gravitational pull on the satellite is modeled, and given satellite insertion parameters, the satellite orbit takes its shape. Only a simple implementation of Orbital Dynamics was

necessary for the attitude studies, and orbit decay and precession were not modeled.

Orbital Dynamics is not the main concern of this work. Several research and commercially available tools are available that perform high fidelity calculations using proven orbit propagation models that calculate orbital changes across the lifetime of the satellite. Since the focus of this work is Attitude Propagation, a simple gravity model was considered to be sufficient to study the attitude behavior over a small number of orbits.

3.1.1 Gravitational Pull

Gravitational force due to Earth acting on the satellite in the nadir direction can be expressed as:

$$F = G \frac{m_{earth} m_{sat}}{r^2}$$

Where G is the gravitational constant
 r is the distance from the center of Earth to the satellite
 m_{earth} is the mass of Earth
 m_{sat} is the mass of the Satellite

The gravitational force the satellite experiences is a function of the position in orbit at a certain time. It acts towards nadir, whose vector rotates as the satellite moves through orbit, and is only constant for perfectly circular orbits. The magnitude of the gravitational force vector oscillates for elliptical orbits as the orbit altitude cycles between its peak and minimum values throughout the orbit.

Figure 3-3 shows the implementation of gravitational attraction in Simulink®. The Force is required by the body dynamics modeling to be in the ECI reference frame. The computations in the Simulink® model can be summarized as:

1. The magnitude of the acceleration due to gravity is calculated given the position of the satellite in ECI

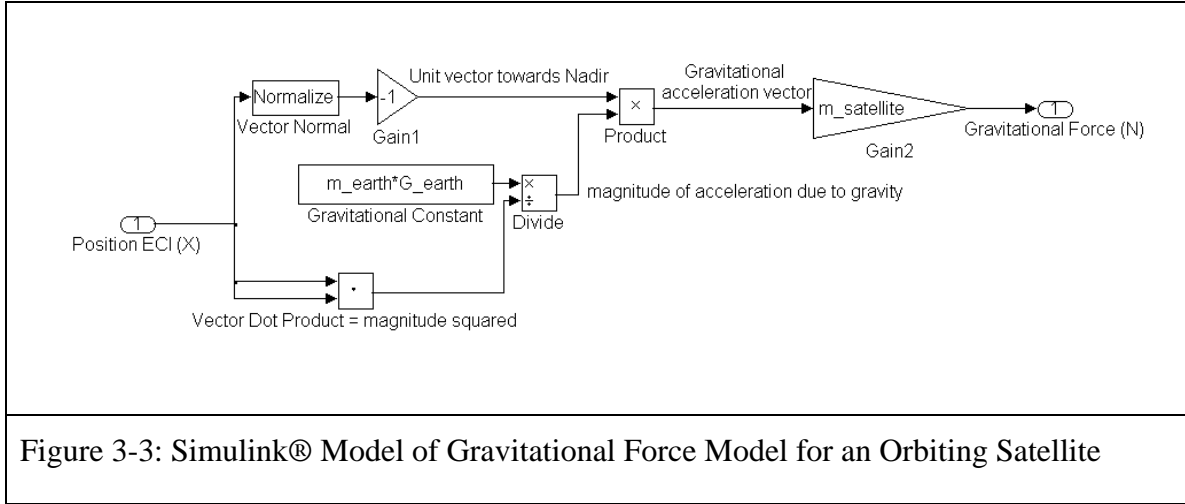
$$Acceleration = \frac{G * m_{earth}}{r^2} = \frac{G * m_{earth}}{\mathbf{X}_{ECI} \cdot \mathbf{X}_{ECI}}$$

2. The unit nadir vector is found from the position vector in ECI

$$\text{Nadir Vector} = -\frac{\mathbf{X}_{\text{ECI}}}{\|\mathbf{X}_{\text{ECI}}\|}$$

3. The vector gravitational acceleration in ECI is then calculated and multiplied by the mass of the satellite to compute the force acting on the satellite.

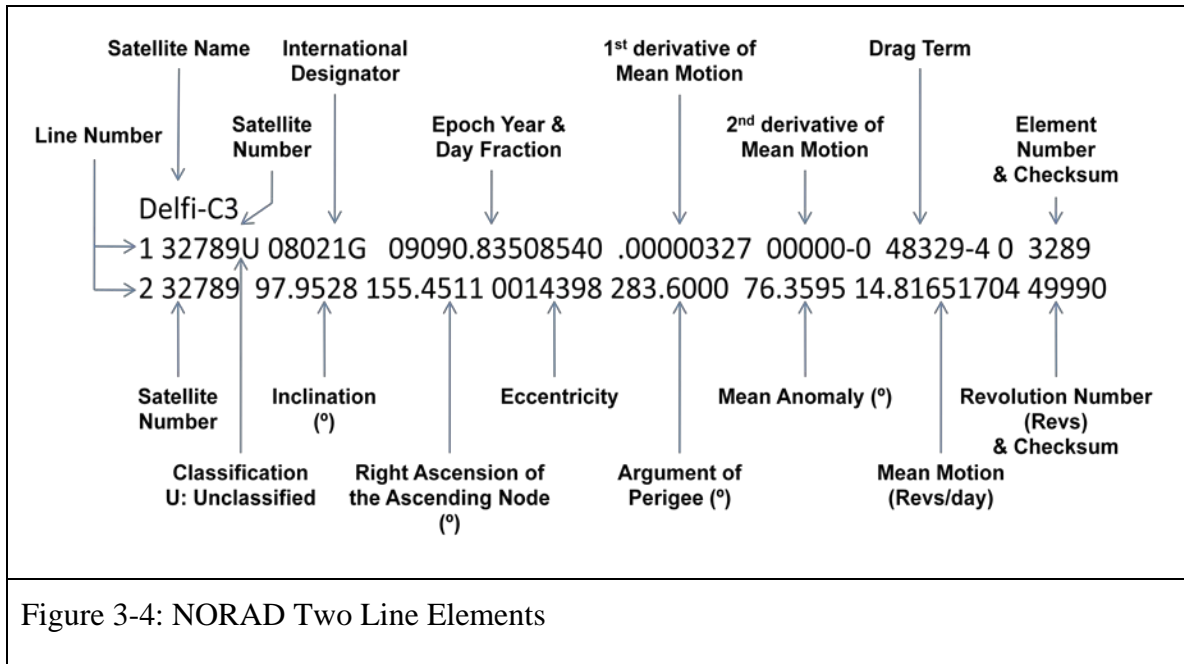
$$\text{Gravitational Force} = \text{Acceleration} * \mathbf{Nadir} * \text{Satellite Mass}$$



3.1.2 Keplerian Elements

A satellite's orbit is normally defined by its Keplerian Elements [2]. NORAD and NASA use a standard form to describe an orbiting satellite known as Two Line Elements (TLE). The implemented orbit propagator uses TLEs to extract initial conditions for the simulations.

Two Line Elements have the form described in Figure 3-4. They include motion parameters that completely define an orbit and can be used to identify the position of the satellite at a given time. Ground station tracking software uses TLEs to predict satellite passes and automated antenna pointing.



In the orbit propagator, the initial conditions (position in orbit, and velocity vector) are extracted from TLEs and fed into the simulation [2]. With the gravitational model, the position of the satellite is propagated and dynamically calculated. This provides a basis for future development to include atmospheric drag, and gravitation from other stellar objects.

3.2 Torque Models

The Orbital Environment Simulator includes four sources of angular moments that affect the satellite. The formulation and modeling of these effects is discussed in detail in this section.

3.2.1 Aerodynamic Drag

At altitudes near the Kármán line (100 km), the Knudsen number typically begins to exceed 1 indicating that the atmosphere more accurately corresponds to a rarefied, free molecular flow regime than a continuum flow regime[11]. Therefore, continuum

Computational Fluid Dynamics (CFD) methodologies cannot be used to study satellites in LEO. Instead, an approach based on free molecular aerodynamics or direct simulation of individual atmospheric particles on the satellite is necessary.

The Atmosphere plays a major role in orbit decay and orbit life. These translational forces due to atmospheric drag cause a decrease in velocity that decreases the altitude of the satellite, until reentry. The majority of literature on atmospheric effects on satellites studies the effects on orbital dynamics. However, atmospheric drag also induces angular moments for asymmetric spacecraft, which is the greater concern in attitude dynamics. Passive stability can be used to achieve a ram-facing steady state utilizing atmospheric drag as discussed in chapter 4.

Atmospheric drag for CubeSats becomes a prominent source of disturbance and angular moments in the low part of LEO, at altitudes of 500km and below. The atmospheric density decreases exponentially as a function of altitude, and atmospheric drag effects become minimal at higher altitudes. The angular moment due to atmospheric drag can be calculated by [3][12]:

$$\mathbf{M}_{aero} = \frac{1}{2} \rho V^2 C_d A (\mathbf{u}_v \times \mathbf{s}_{cp})$$

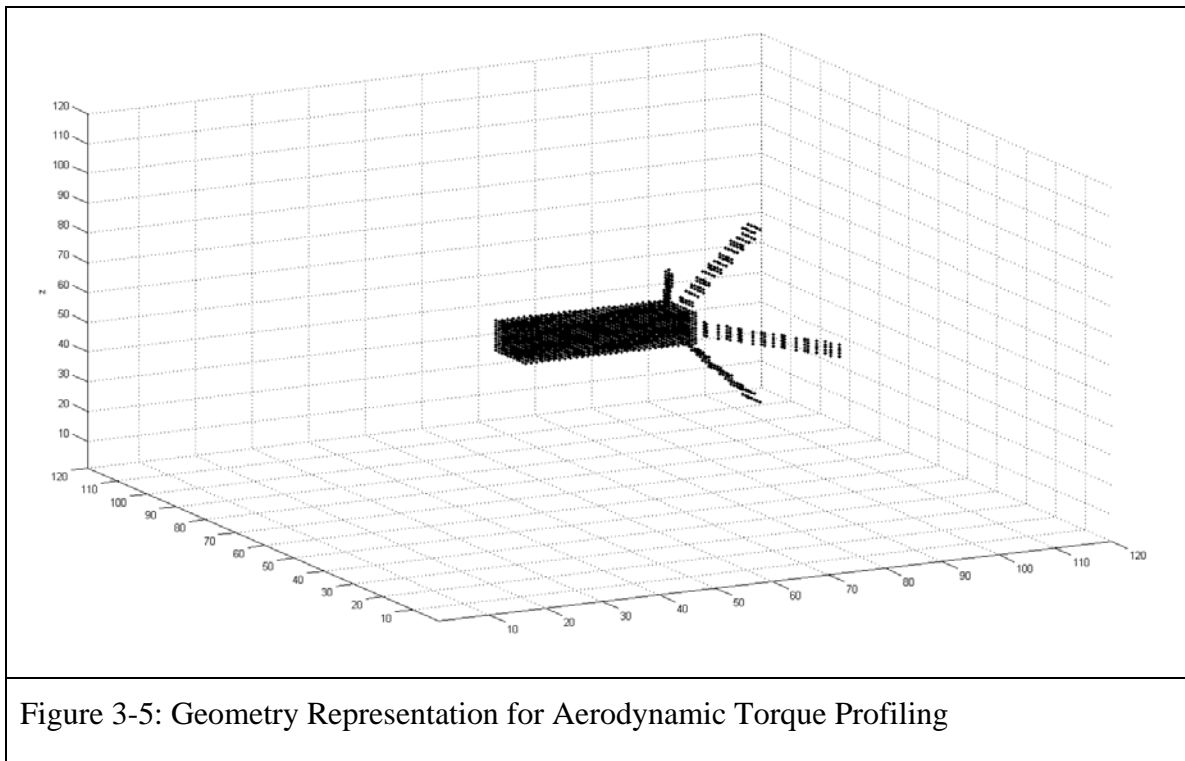
Where

- \mathbf{M}_{aero} is the aerodynamic torque
- \mathbf{u}_v is the unit velocity vector
- \mathbf{s}_{cp} is the vector from the center of pressure to the center of mass
- ρ is the atmospheric density
- V is the satellite velocity
- C_d is the drag coefficient
- A is the affected area

3.2.1.1 Aerodynamic Geometric Representation

The aerodynamic torque for a certain attitude is a function of the area facing the velocity vector that is not shadowed by any other parts of the spacecraft body. Taking torque due to aerodynamics into account requires some form of representation of the spacecraft geometry. Then an algorithm is needed to calculate the torque the spacecraft experiences given the geometric representation, and the attitude of the satellite relative to the velocity vector.

The description of the satellite for aerodynamic calculations is more challenging than it is to describe the magnetic characteristics for magnetic calculations, or the mass distribution for gravity gradient purposes. The geometry of the satellite is discretized into volumetric elements as shown in Figure 3-5. The satellite in Figure 3-5 is a 3U CubeSat with side panels that deploy into a shuttlecock configuration. The aerodynamic stability of this configuration is discussed in detail in Chapter 4.



To compute the aerodynamic torque, an algorithm is implemented to find the satellite elements directly facing the wind vector. This is a simple method to account for

shadowing of parts of the satellite over others. Shadowing is often ignored in literature when the main body of the satellite is small relative to the size and length of the fins, but as a general solution and to study arbitrarily shaped satellites where the response is unpredictable, shadowing is an important factor to consider.

Using the equation which was described in detail above

$$\mathbf{M}_{\text{aero}} = \frac{1}{2} \rho V^2 C_d A (\mathbf{u}_v \times \mathbf{s}_{cp})$$

the aerodynamic effect is calculated at discretized area elements on the satellite that are facing the wind vector and accumulated to find the collective effect, essential being a form of numerical integration over the entire area. It was found that to compute the collective torque affecting the satellite at each time step of the simulation given the attitude is computationally extensive and requires a significant amount of time. This issue motivated the creation of Torque Profiles, to reduce the attitude propagation simulation time. Once the satellite has been geometrically characterized as in Figure 3-5, the implemented algorithm creates a lookup table of torque values as a function of the attitude relative to the wind.

The Torque Profile is a two dimensional lookup table created by rotating the satellite 0° to 45 ° in roll, and 0 ° to 180 ° in pitch for each roll angle and calculating the collective torque due to the atmosphere on the satellite at each attitude. The angle ranges over which the lookup table is generated is sufficient to find the torque affecting the satellite at any attitude.

3.2.1.2 Aerodynamic Torque Modeling

The Simulink implementation of aerodynamic moments within the attitude propagator takes the Velocity, Attitude, and Position of the satellite in orbit as inputs. The position in orbit is only required to calculate the altitude to find the atmospheric density at that point. The velocity vector is used in the vector calculations to compute the torque vector affecting the satellite. The magnitude of the torque is also proportional to the square of

the velocity.

The model can be thought of in two parts; calculating the magnitude of the torque given the attitude, altitude, and velocity, and finding the torque unit vector given the orientation of the satellite relative to the wind vector. Figure 3-6 is a screenshot of the Simulink implementation.

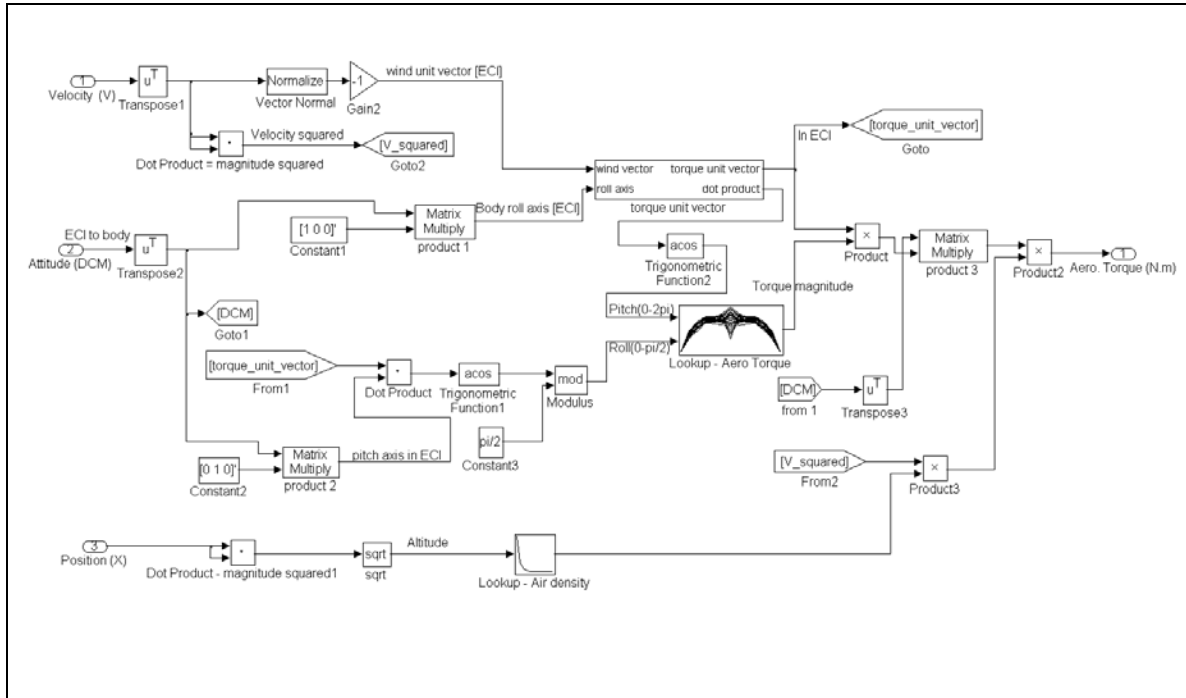


Figure 3-6: Simulink® Model of Aerodynamic Torque

The computations in the Simulink® model can be summarized as:

1. The roll and pitch axes (S_x and S_y) in body frame are rotated to ECI, to perform all computations in ECI

$$S_{x_{ECI}} = C_{ib} S_{x_{body}}$$

$$S_{y_{ECI}} = C_{ib} S_{y_{body}}$$

2. The unit torque vector is found given the wind unit vector, and S_x (roll axis)

$$\|M_{aero}\| = \|-V\| \times \|S_x\|$$

3. To retrieve the torque from the lookup table, the pitch angle is calculated as the

angle between the wind vector and the roll axis

$$pitch = \cos^{-1}(\|\mathbf{Sx}\| \cdot \|\mathbf{-V}\|)$$

4. The roll angle is calculated as the angle between the torque unit vector and the satellite pitch axis, modulo $\pi/2$

$$roll = \cos^{-1}(\|\mathbf{M}_{aero}\| \cdot \|\mathbf{Sy}\|) \pmod{\frac{\pi}{2}}$$

5. Using the roll and pitch angles, the magnitude of the torque can now be calculated as

$$\mathbf{M}_{aero} = M_{lookup} \rho V^2 \|\mathbf{M}_{aero}\|$$

where a lookup table is used to find the atmospheric density ρ as a function of altitude, and V is the velocity of the satellite in orbit that is dynamically calculated at each time step.

6. Finally, the aerodynamic torque is rotated into the body frame

$$\mathbf{M}_{body} = \mathbf{C}_{bi} \mathbf{M}_{ECI}$$

3.2.1 Gravity Gradient

Gravity Gradient torque is a significant source of angular moments in LEO. The gravity gradient torque for an earth orbiting satellite is caused by differences in the distance to earth across the satellite body; mass that is closer to Earth experiences higher gravitational attraction. For a given satellite geometry the torque profile due to the gravity gradient is a function of attitude. An asymmetric body in a gravitational field will experience a torque tending to align the axis of least inertia with the field direction [13].

The Gravity Gradient angular moment can be calculated as [3][12]:

$$\mathbf{M}_{gg} = \frac{3\mu}{R_0^3} \mathbf{u}_e \times \mathbf{J} \mathbf{u}_e$$

Where \mathbf{M}_{gg} is the gravity gradient torque

- \mathbf{u}_e is the unit vector towards nadir
- R_0 is the distance from the center of Earth to the satellite
- J is the inertia matrix
- μ is the geocentric gravitational constant

For the case of CubeSats without deployable components, the 3-U variants experience the most gravity gradient moments due to their mass distribution. The length of the satellite will tend to line up with Nadir.

3.2.1.1 Gravity Gradient Modeling

In order to calculate the gravity gradient torque affecting a satellite at an instant in time, the position in orbit, attitude, and mass properties of the satellite are required. The distance to earth R_0 and the nadir vector \mathbf{u}_e can be calculated at a given point from the position in ECI. The attitude of the satellite is also required to transform the nadir vector from ECI to body-frame, in order to calculate the effective torque in body-frame.

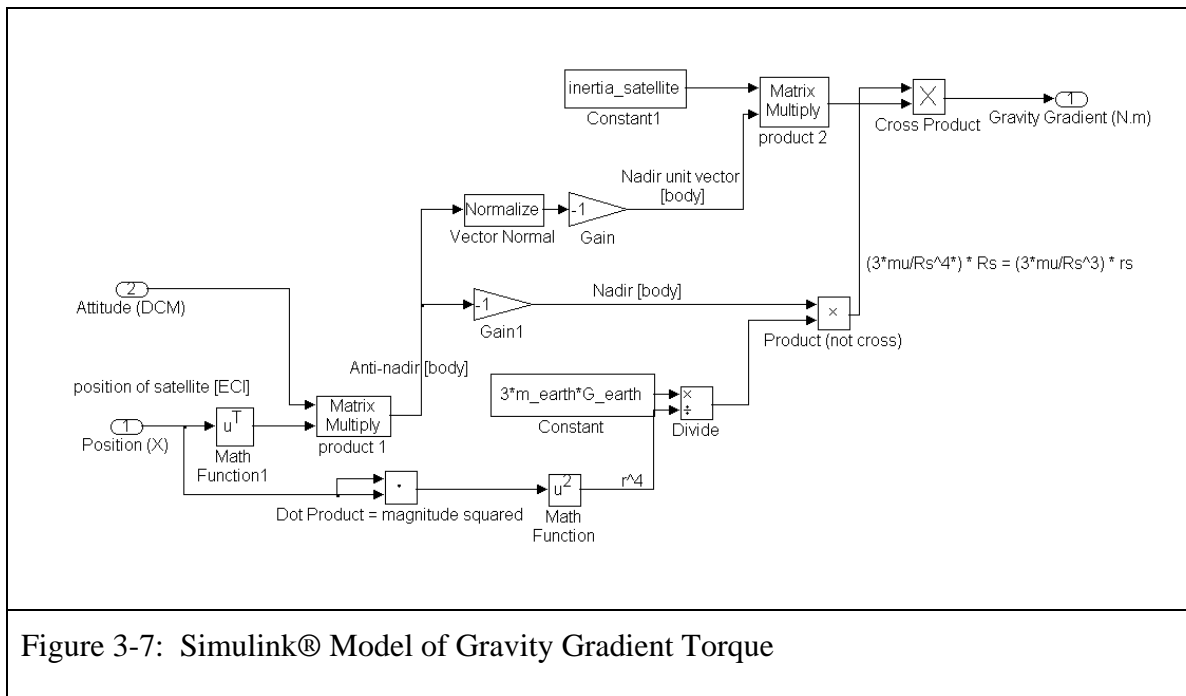


Figure 3-7: Simulink® Model of Gravity Gradient Torque

The computations in the Simulink® model can be summarized as:

7. The position vector is first rotated into body frame

$$\mathbf{X}_{body} = \mathbf{C}_{bi} \mathbf{X}_{ECI}$$

8. The left side of the cross-product is computed given a set defined constants, and the position in ECI

$$\frac{3\mu}{R_0^3} \mathbf{u}_e = \frac{3 * G * m_{earth}}{(\sqrt{\mathbf{X}_{ECI} \cdot \mathbf{X}_{ECI}})^3} \mathbf{u}_e = \frac{3 * G * m_{earth}}{(\mathbf{X}_{ECI} \cdot \mathbf{X}_{ECI})^2} * -\mathbf{R}_0$$

In order to reduce the number of computations, the square-root and vector normalization procedures were avoided by increasing the power in the denominator to 4 (to perform a sequence of two dot-products instead), and leaving the Nadir vector with a magnitude that equals the distance to the center of Earth to.

9. The cross product is computed, factoring in the inertia matrix, to calculate the torque vector in body frame due to gravity gradient.

3.2.1.2 Gravity Gradient Stabilization

Previous work on the use of Gravity Gradient moments for satellite stabilization is highlighted in section 2.3.1. The approach involves deployable gravity gradient booms that change the mass distribution to a configuration that experiences gravity gradient moments greater than other expected disturbance torques, causing it to become stable in a nadir-pointing attitude.

With Gravity Gradient being modeled in the Attitude Propagator, evaluating the performance of a stability system of a small satellite with gravity gradient bias is a simple task. This thesis however does not include a chapter on Gravity Gradient stabilization because it has not yet been a focus of a satellite design within the Kentucky Space program.

From simple test runs, a combination of an inertia bias (mass distributed such that one axis has smaller moment of inertia than the other two orthogonal axes) and hysteresis damping, a nadir pointing behavior was observed, at the expected accuracies between 10° and 20° of error.

3.2.2 Magnetic Torques

A magnetic dipole in a magnetic field experiences an angular moment that aligns the dipole with the magnetic field lines, like a compass needle pointing north. Magnetic dipoles occur in spacecraft transiently from the on-board electronics especially high-current modules such as radios. The structure of the spacecraft may contain a residual dipole that can also be a source of unwanted disturbance angular moments.

Magnetic effects can also be used to control and stabilize the attitude of a satellite. Passive magnetic stabilization, as discussed in chapter 5, utilizes a set of permanent magnets to align the satellite with the Earth’s magnetic field and prevent random tumble. Magnetically “soft” material of low coercivity is easily magnetized by the Earth’s magnetic field and follows hysteresis patterns that make it suitable as a means for angular rate damping to accompany various control techniques. Magnetic hysteresis material contains magnetic dipoles that create angular moments by interacting with the magnetic field, ultimately resulting in the damping effect.

Active attitude control can be achieved by using magnetic torque rods or torque coils. Mounting current coils orthogonally in the satellite, controlled magnetic dipoles can be induced to stabilize a satellite and perform slew maneuvers.

The torque produced by a magnetic dipole is calculated as [13]:

$$\mathbf{M}_{\text{magnetic}} = \mathbf{m} \times \mathbf{B}_{\text{earth}}$$

Where \mathbf{M} is the magnetic torque
 \mathbf{m} is the magnetic dipole moment in Am^2
 $\mathbf{B}_{\text{earth}}$ is the Earth magnetic flux density vector

Since the relationship involves a cross-product, angular moments parallel to the external magnetic field cannot be generated by permanent magnets, nor in a controlled torque coils system. In other words, a dipole tends to line up with the external magnetic field, but it spins freely about the magnetic field vector causing an uncontrolled axis of rotation.

The magnetic dipole for a current coil is:

$$\mathbf{m} = I n \mathbf{A}$$

Where \mathbf{m} is the magnetic dipole in Am^2
 I is the current through the coil
 n is the number of turns.
 A is the area of the coil

For a permanent magnet, or any material, the magnetic dipole can be calculated as:

$$\mathbf{m} = \frac{\mathbf{B}V}{\mu_0}$$

Where \mathbf{m} is the magnetic dipole in Am^2
 B is the magnetic flux density of the magnet
 V is the volume of the material
 μ_0 is the permeability of free space

3.2.2.1 Magnetic Field Dipole Model

The earth's magnetic field can be modeled by a magnetic dipole at the Earth's core. There are other magnetic models such as the Spherical Harmonic Model, and others based on measured data, provide more accurate descriptions of the magnetic field strengths and directions. The more accurate models also require greater computational resources, so the Dipole Model (also called the L-Shell magnetic field model) is used in the attitude propagator.

Approximating the Earth's magnetic field as an ideal dipole is sufficient for simulation purposes in most applications. More accurate models become necessary in the spacecraft-implementation of attitude determination systems that use the magnetic field measurements along with orbital information to deduce the satellite's attitude.

The magnetic North pole is located in the southern hemisphere, and the magnetic dipole is not aligned with the Earth's spin axis. The magnetic dipole also experiences changes in orientation and strength with time. In 1978, the magnetic dipole's longitude was 109.3° and latitude was 168.6° [3]. It is noted that the magnetic dipole is fixed in the ECEF frame, and rotates with respect to the ECI frame.

Based on the development of the Dipole Model in [3], the magnetic field at a certain point in orbit can be calculated as:

$$B(\mathbf{X}) = \frac{a^3 H_0}{\|\mathbf{X}\|^3} [3(\mathbf{u}_m \cdot \mathbf{u}_x)\mathbf{u}_x - \mathbf{u}_m]$$

| | | |
|-------|----------------|-----------------------------------------------------------------------|
| Where | a | is the equatorial radius of Earth in meters |
| | H_0 | is the dipole strength in $Wb \cdot m$ |
| | \mathbf{u}_m | is the unit vector along the magnetic dipole |
| | \mathbf{u}_x | is the unit position vector at which the magnetic field is calculated |

Since the magnetic dipole is in ECEF, it is convenient to compute the magnetic field in that reference frame, and then convert it to ECI. In order to perform the calculation in

ECEF, the position in orbit given in ECI must first be rotated to ECEF.

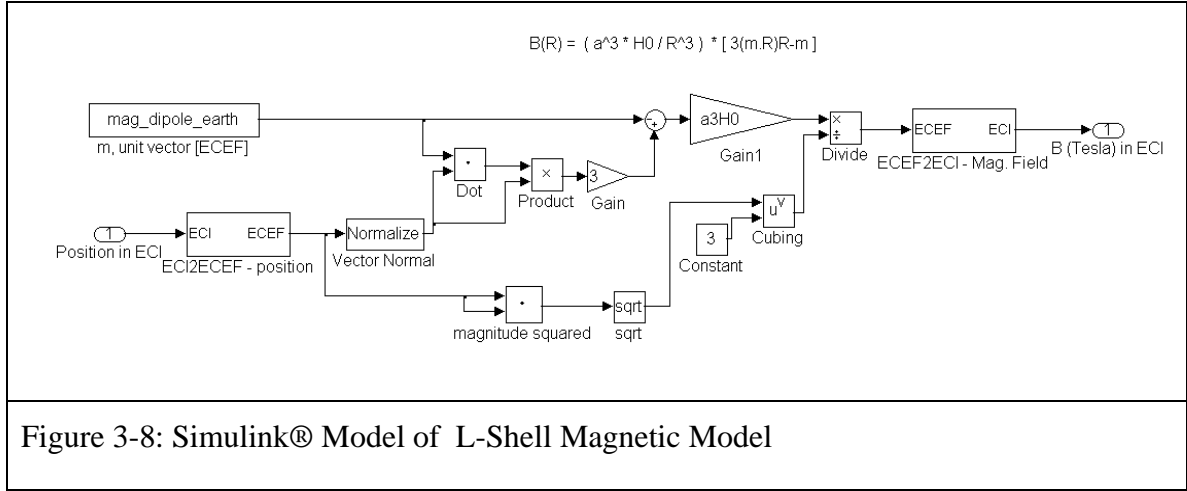


Figure 3-8: Simulink® Model of L-Shell Magnetic Model

The computations in the Simulink® model can be summarized as:

1. The position vector is first rotated into ECEF

$$\mathbf{X}_{ECEF} = \mathbf{C}_{ei} \mathbf{X}_{ECI}$$

\mathbf{C}_{ei} is time dependent as the ECEF frame rotates about ECI.

2. The magnetic field is computed, in ECEF, as

$$B(\mathbf{X}) = \frac{a^3 H_0}{\|\mathbf{X}\|^3} [3(\mathbf{u}_m \cdot \mathbf{u}_x) \mathbf{u}_x - \mathbf{u}_m] = \frac{a^3 H_0}{(\sqrt{\mathbf{X} \cdot \mathbf{X}})^3} [3((\mathbf{u}_m \cdot \mathbf{u}_x) \mathbf{u}_x) - \mathbf{u}_m]$$

3. Finally, the calculated value of the magnetic field is rotated to ECI, and returned to the parent model

$$\mathbf{B}_{ECI} = \mathbf{C}_{ie} \mathbf{B}_{ECEF}$$

The L-Shell magnetic model is used in other modules that calculate the torque due to permanent magnets, and the behavior of hysteresis material.

3.2.2.2 Magnetic Torque Model

The magnetic torque component of the attitude propagator calculates the torque due to permanent magnets mounted into the satellite structure by design. This is primarily used to simulate passive magnetic stabilization where the goal is that the satellite tracks or

aligns with the earth's magnetic field in its orbit.

In order to calculate the torque affecting the satellite in body-frame due to permanent magnets placed in the satellite, the calculations in the Simulink® implementation are performed in body-frame. The value of the earth's magnetic field retrieved from the L-Shell model, is rotated using the DCM describing the attitude from ECI to body-frame.

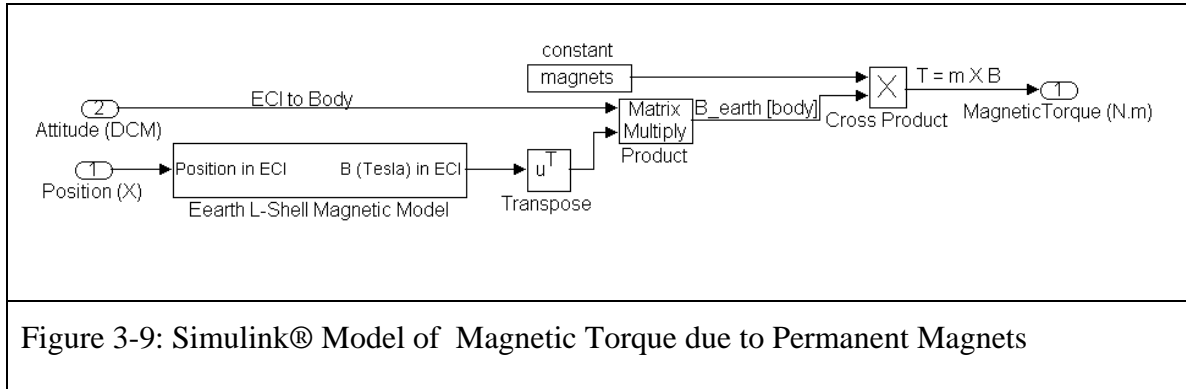


Figure 3-9: Simulink® Model of Magnetic Torque due to Permanent Magnets

The Simulink® model of Magnetic Torque due to permanent magnets performs the cross product in body frame. The magnetic field at a certain point in orbit is calculated by the earth L-Shell model as illustrated in the previous section, and the torque is then calculated as

$$\mathbf{M}_{\text{magnetic}} = \mathbf{m} \times \mathbf{B}_{\text{earth}}$$

Where m is the magnetic dipole moment of the permanent magnets placed in the satellite, it's a constant in the simulation and a part of the predefined description of the satellite. B_{earth} is rotated into body frame before performing the cross product, in order to express the calculated torque in body frame.

3.2.3 Magnetic Hysteresis Material Angular Rate Damping

Angular rate damping is a major problem in satellite attitude dynamics. The nature of the space environment is such that there is almost no friction (or damping), i.e. torques proportional to the angular rate of the satellite opposing rotations are minimal. In a systems sense, passive stabilization behaves as a second order system with a very low damping factor. The concept can be pictured as a pendulum in vacuum oscillating

endlessly, or as a spring mass system without friction.

As discussed in the previous sections, a gravity gradient stabilized satellite oscillates around the nadir vector, an aerodynamically stabilized satellite oscillates about the velocity vector, and a magnetically stabilized satellite oscillates around the magnetic field lines in orbit. A form of angular damping must be included in the satellite design in order to achieve the oscillatory steady state. Gravity gradient and permanent magnets do not provide any form of energy dissipation, and aerodynamic drag provides a minimal amount that is negligible. Specifically the magnitude of the torque due to the angular motion is approximately four orders of magnitude smaller than the main torque component caused by aerodynamic drag [3].

Angular rate damping can be achieved using active reaction wheels or magnetic torque coils, by countering the angular rotations measured using an onboard gyroscope. Such a feedback system increases the power and computation requirements and comes with the added complexity and risk of an active attitude control system.

One way to achieve angular rate damping passively is by simply adding magnetic hysteresis material. Magnetic hysteresis is the phenomena of energy loss in material in a cycling magnetic field to flips in magnetic domains in the material, which are not frictionless. Material with low enough coercivity H_c to be magnetized and demagnetized by the Earth's magnetic field is required. Also, a high permeability increases the effectiveness of the hysteresis. Figure 3-10 shows a typical magnetic hysteresis curve. H_c is the coercivity, B_r is the remanence, and B_s is the saturation magnetic flux density. As H cycles as the satellite rotates through a magnetic field, the material magnetizes and demagnetizes along the hysteresis curve. The area inside the hysteresis loop is the energy lost as heat for a given cycle.

3.2.4 Magnetic Hysteresis Modeling

Magnetic hysteresis is a physical property of ferromagnetic material. The material

becomes magnetized when an external magnetic field is applied forcing the magnetic domains on the atomic level to polarize. Depending on the magnetic remanence of the material, it will retain a magnetic dipole of some strength when the external magnetic field is removed. Figure 3-10 shows a typical magnetization curve of ferromagnetic material along with the Simulink Model that approximates the behavior.

The magnetic coercivity of the material is the intensity of the external magnetic field applied against the polarity of the material required to diminish the magnetization to zero after it has been driven to saturation. The lag (or “Hysteresis”) in tracking the externally applied magnetic field caused by the coercivity and remanence of the ferromagnetic material results in energy lost as heat in the material. The phenomenon can be thought of as the magnetic dipoles having “friction” when their orientation changes.

As mentioned in section 3.2.3, magnetic hysteresis material, when chosen with low enough coercivity that the Earth’s magnetic field is sufficient to magnetize and demagnetize it, is an effective angular rate damping method for light weight satellites. It is also a completely passive and simple solution; it is only required to include a calculated amount of hysteresis material on board the satellite to achieve damping.

Quantifying the amount of hysteresis material to include in a satellite design is challenging. The amount of damping caused by hysteresis material is not a fixed or calculated amount, it is a result of the behavior of the hysteresis material interacting with the Earth’s magnetic field. Modeling and simulation is a convenient and effective way to study hysteresis material[9].

The green curve in Figure 3-10 represents the approximation implemented in Simulink. The model fairly accurately simulates the behavior when the hysteresis material is driven to saturation in each direction with every cycle of the external magnetic field. However accuracy is lost when the satellite stabilizes and the material response oscillates in a smaller hysteresis loop contained within the full loop, since only the full loop is modeled. In that case, hysteresis does not occur anymore and the material response would track one

of the two curve branches.

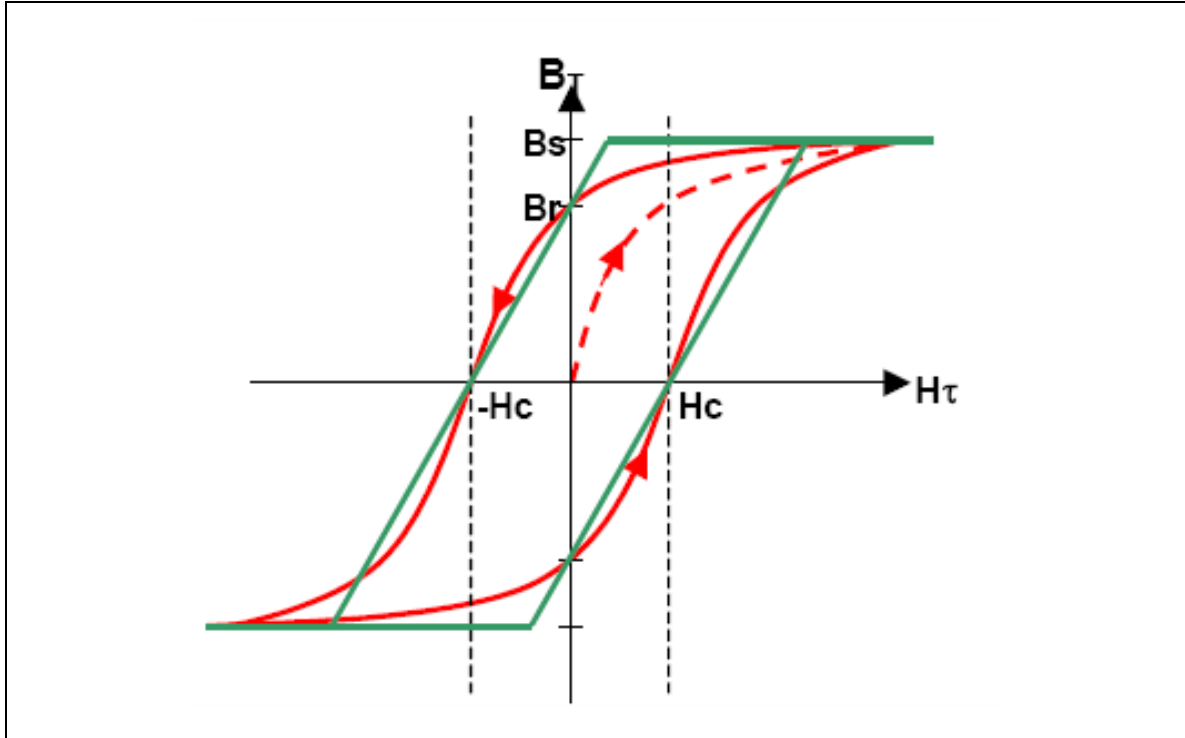


Figure 3-10: Hysteresis loop modeling in Simulink® [9]

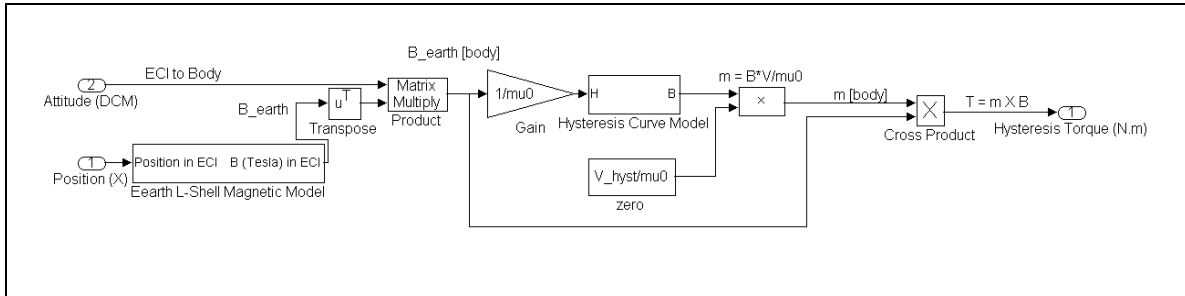


Figure 3-11: Simulink® Model of Magnetic Torque due to Hysteresis Material

The computations in the Simulink® model can be summarized as:

1. The Earth's magnetic field density at the satellite's location is calculated using the L-Shell model, which is described in detail in section 3.2.2.1. The vector is rotated into body frame using the transformation

$$\mathbf{B}_{Earth_{body}} = \mathbf{C}_{bi} \mathbf{B}_{Earth_{ECI}}$$

\mathbf{C}_{bi} is the rotation matrix from the ECI frame to the body frame describing the attitude of the satellite.

2. The magnetic field intensity (the magnetizing field) is computed as

$$\mathbf{H}_{Earth} = \frac{1}{\mu_0} \mathbf{B}_{Earth}$$

3. The magnetic field density is computed using the approximated Hysteresis Loop model described above

$$\mathbf{B}_{hysteresis\ material} = \text{Hysteresis Curve}(\mathbf{H}_{Earth})$$

4. The magnetic moment of the hysteresis material is found next as

$$\mathbf{m}_{hysteresis} = \frac{\mathbf{B}_{hysteresis\ material} V_{hysteresis}}{\mu_0}$$

where $V_{hysteresis}$ is the volume of the hysteresis material along the three axes.

5. Finally, the torque is calculated as the cross product of the magnetic moment of the hysteresis material $\mathbf{m}_{hysteresis}$ and the Earth's magnetic field density \mathbf{B}_{earth}

$$\mathbf{M}_{hysteresis} = \mathbf{m}_{hysteresis} \times \mathbf{B}_{Earth}$$

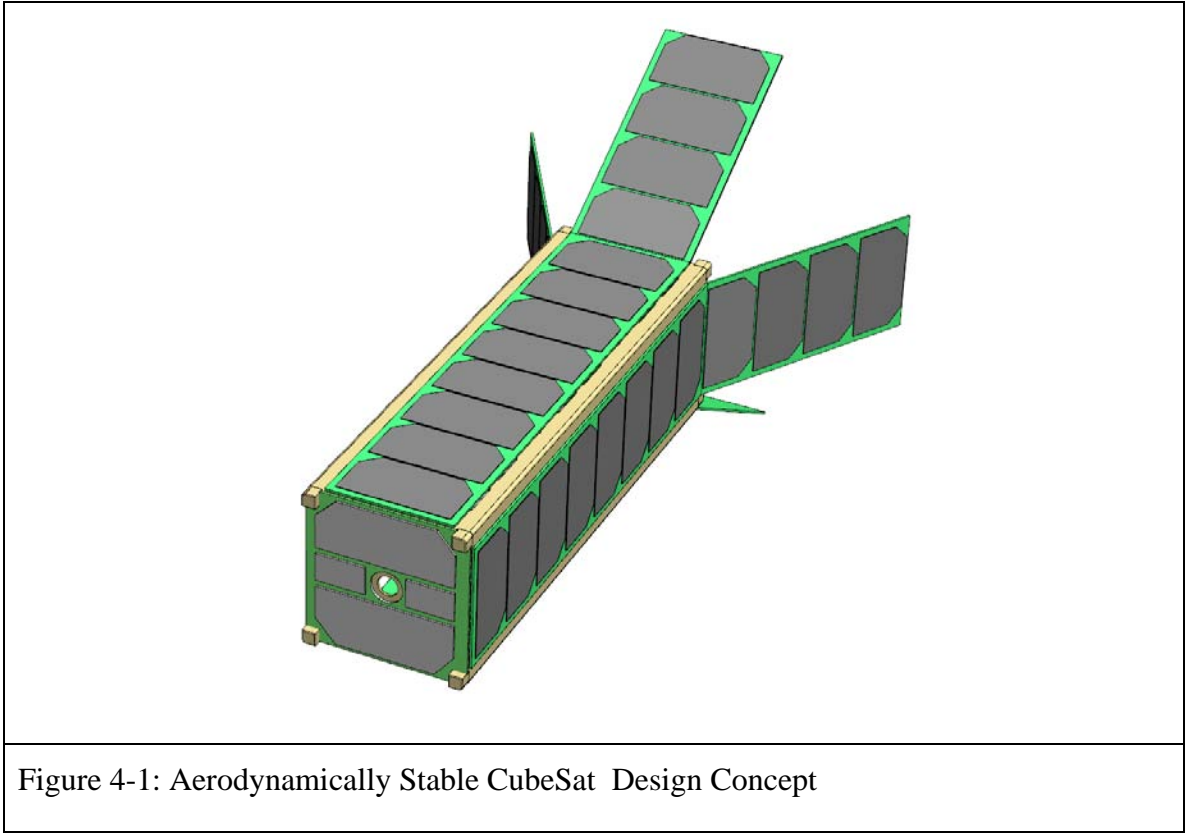
4 Aerostabilized CubeSat Design

This chapter describes the design, modeling, and analysis of an attitude control system for a ram-facing pico-class satellite in Low Earth Orbit (LEO). A 3-U (30x10x10 cm³) CubeSat is designed to maintain one 10x10 cm² face normal to the velocity vector throughout the orbit. The solution presented implements deployable drag fins and resembles a shuttlecock design which is shown to be capable of providing passive stabilization for orbits below 500 km. The attitude propagator described in this thesis is used to observe the satellite's dynamic response and steady-state behavior due to aerodynamic torques while considering perturbing torques due to gravity gradient and magnetic effects. Stability characteristics and pointing errors are shown for altitudes ranging from 300 to 450 km with fin lengths from 2 to 30 cm at angles from 0 to 90 degrees.

4.1 Design Concept

The objective is to carry an atmospheric sensor on the front face which requires its aperture to track the velocity vector. The satellite is in a 3-U CubeSat configuration that measures 10x10x30 cm³ before deployment and weighs less than 5 kg with the center of mass at the geometric center during launch. The satellite is required to recover from the initial tumble after launch then achieve and maintain a ram-facing steady-state attitude. In this configuration, the satellite will perform one revolution about the pitch axis per orbit.

The design and simulations presented are based on a 3-U CubeSat with deployable side panels resembling a badminton "shuttlecock". Stability is achieved by placing the center of drag pressure behind the center of mass. Figure 3-1 shows the configuration of the satellite where side panels are deployed to a narrow angle measured from the negative velocity vector (See Figure 4-2). The panel deployment angle, the length of the deployable side panels, and the orbit altitude were varied and simulated to analyze the effect of these variables on the steady-state behavior of the satellite.



Section 2.3.2 discusses related research and results from previous experiments for geometries similar to the one considered here. In the following sections, the aerodynamic torque is studied across the design variables to find stable and disturbance-resilient configurations. The Simulation Results section highlights the response of two satellite designs when simulated in the attitude propagator in orbit under disturbance torques.

4.2 Design Space Analysis in 1-DOF

To study the effect of panel length and panel deployment angle on the behavior in steady state, a cross section of the system was considered to study the dynamics in 1-DOF. Atmospheric modeling and simulations were developed similar to section 3.2.1. The details of this research are developed in [14].

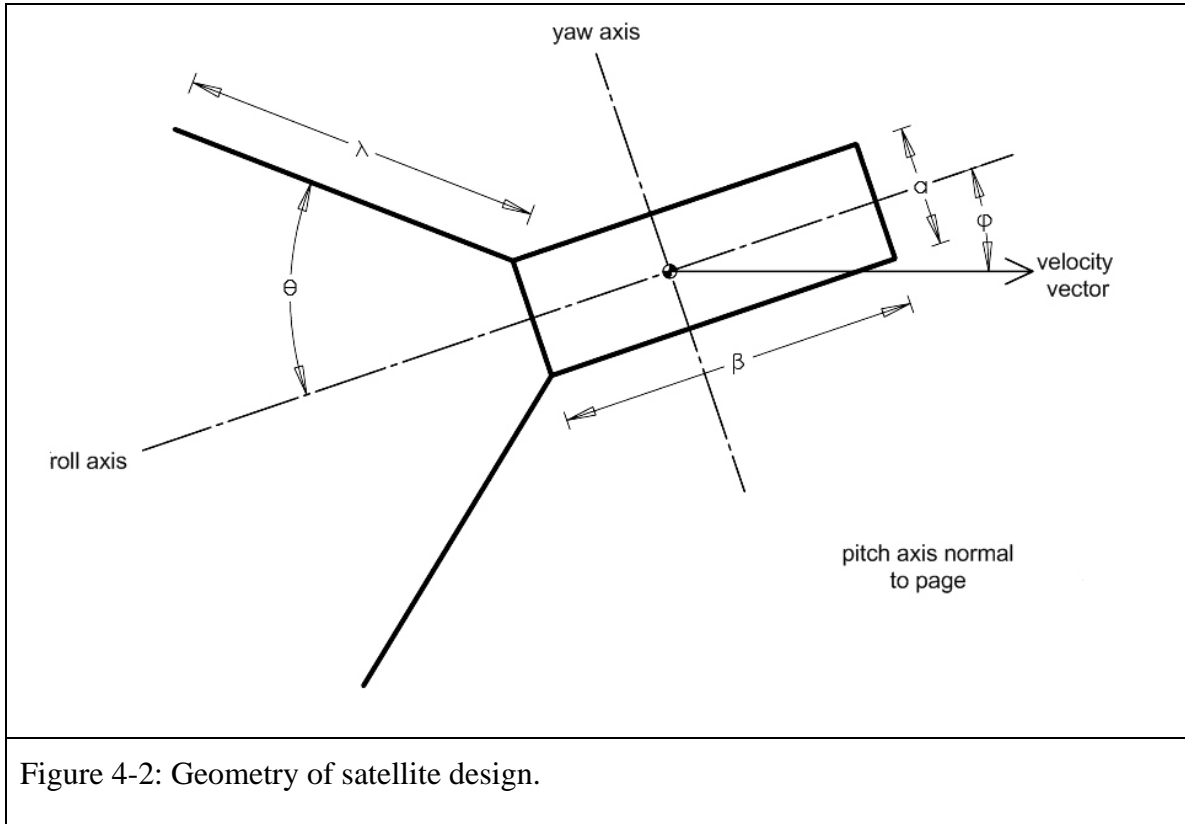


Figure 4-2: Geometry of satellite design.

Figure 4-2 illustrates the geometric variables and the attitude to the velocity vector defined by ϕ . The main body dimensions α and β are constant across the simulations at 10 cm and 30 cm respectively. The deployable panel length (λ) and deployment angle (θ) are the parameters varied to optimize performance. An exhaustive search through the panel deployment angle, panel length, and orbit altitude was performed to determine the optimal deployment angle and panel length.

Pitch Torque Profiles. Figure 4-3 shows a set of torque profiles for three designs with a panel length $\lambda = 20$ cm at different deployment angles $\theta = 10^\circ, 30^\circ$ and 50° at an altitude of 400 km as a function of its attitude to the velocity vector (ϕ). Negative sloped zero-crossings indicate stable points at which the satellite will settle temporarily or permanently; a positive error angle produces negative torque to realign the satellite to the

stable point, and vice-versa.

At shallow deployment angles the shadowing of the drag panels by the satellite main body affects the linearity of the torque profile through the 0 degree pitch angle. At deployment angles greater than 75 degrees, secondary stable points begin to appear near ± 90 degrees pitch, where the projected drag area of the fins perpendicular to the flow begins to diminish and the torque affecting them balances out with the atmospheric drag on the satellite main body.

In general the panel length was found to mainly scale the torque profile in amplitude for panel lengths greater than 10 cm. Likewise, evaluating the torque profiles at lower altitudes with higher atmospheric density increases the torque experienced and is manifested as a scaling in the torque profile.

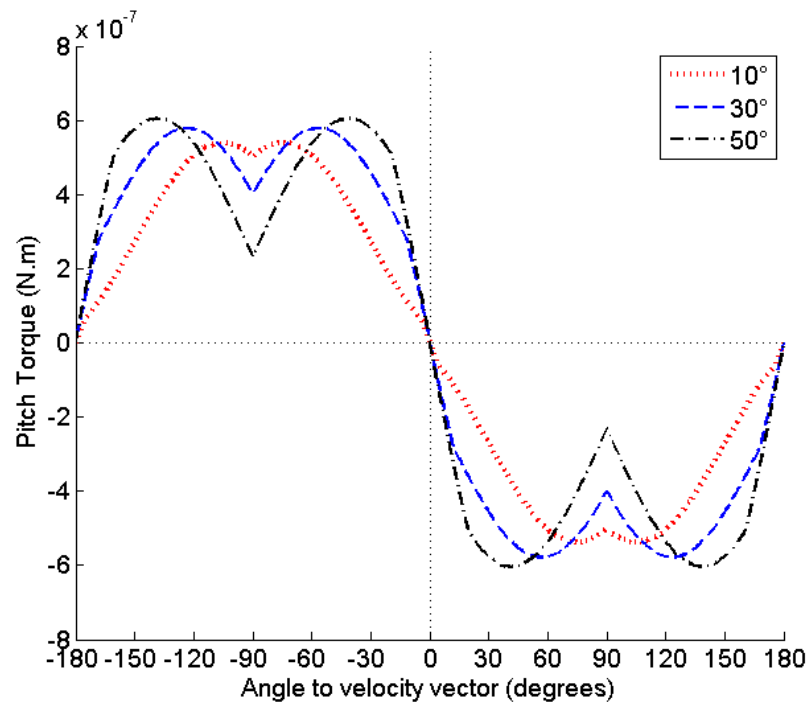


Figure 4-3: Pitch Torque Profiles showing torque experienced as a function of the angle to velocity vector (ϕ)

Stiffness. The main performance parameter considered was the amount of “stiffness” through the ram-facing angle. Stiffness is defined as the amount of correcting torque the satellite experiences for every 1 degree of error, which is calculated as the negative of the derivative of the pitch torque relative to the pitch attitude angle evaluated at the zero degrees pitch angle ($\varphi = 0$). Simulations showed that satellites with greater stiffness resulted in smaller steady state errors and higher oscillation frequencies.

Varying the deployment angle yields an optimal value at which stiffness is greatest for a given panel length. Figure 4-4 illustrates stiffness curves over variable deployment angles for several panel lengths. The most efficient deployment angle is around $\theta = 50$ degrees. The drag area by the satellite with deployed panels has a direct effect on orbit life. Orbit dwell times were calculated to be below 1 year for a wide range of design combinations at altitudes of 400km and below. Therefore, the optimal design for a specific mission is a trade study between the stiffness (pointing accuracy) and orbit life.

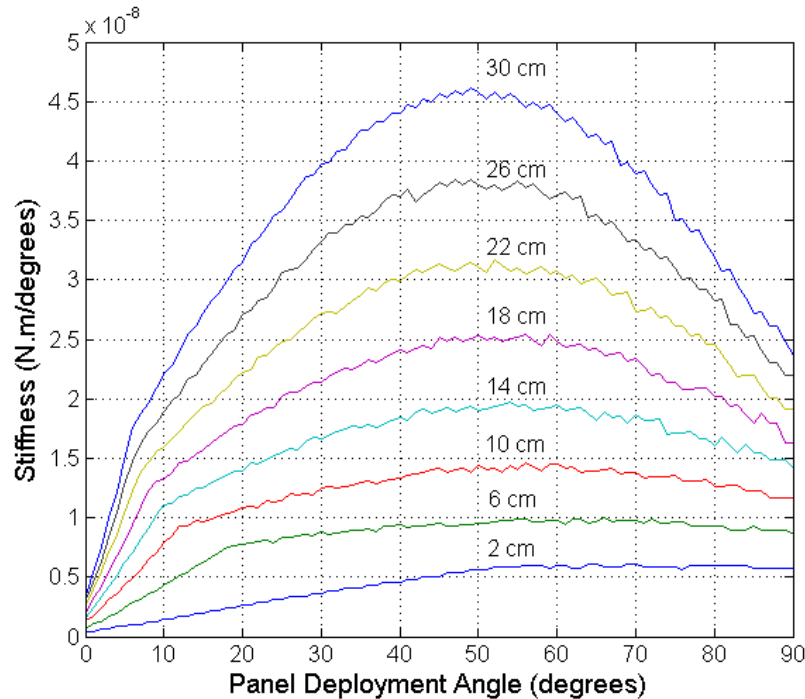


Figure 4-4: Aerodynamic stiffness at 400 km altitude for a range of panel lengths (λ).

Effect on Steady-state Error. Figure 4-5 shows equal-stiffness curves over the geometric design variables the panel length (λ) and the deployment angle (θ). Each curve represents length and angle combinations that have equal stiffness and provide the same steady state performance. The orbit propagator was run on a range of ideal constant aerodynamic stiffness values to correlate them to the resulting steady-state error values. This ideal approximation is valid when the slope of the torque profile spans linearly beyond the range of expected worst case steady-state error. The ideal stiffness values in Figure 4-5 translated to steady state errors of $\pm 2.5^\circ$ to $\pm 31^\circ$. It is not recommended to use values of the deployment angle $\theta < 20^\circ$ where the linearity of the stiffness slope does not span beyond $\varphi = \pm 7^\circ$ from the main stable point.

Altitude. Because the atmospheric density varies exponentially, the achievable steady-state pointing accuracy is highly dependent on the orbit. Figure 4-6 gives insight into the effect of orbit altitude on the achievable steady state. The plot shows the steady-state error as a function of the panel length for panels deployed at $\theta = 50^\circ$ over several altitudes. These plots were obtained using the actual torque profiles with non-ideal stiffness.

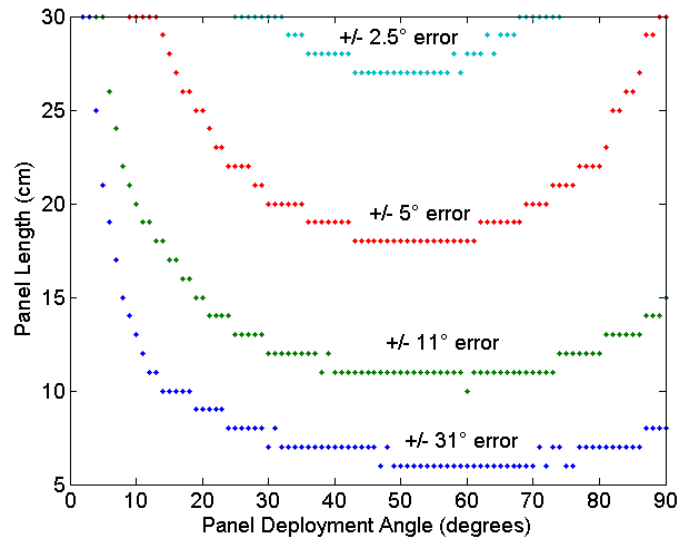


Figure 4-5: Constant stiffness curves at 400km altitude. Panel length (λ) and deployment angle (θ) combinations to obtain equal steady-state performance.

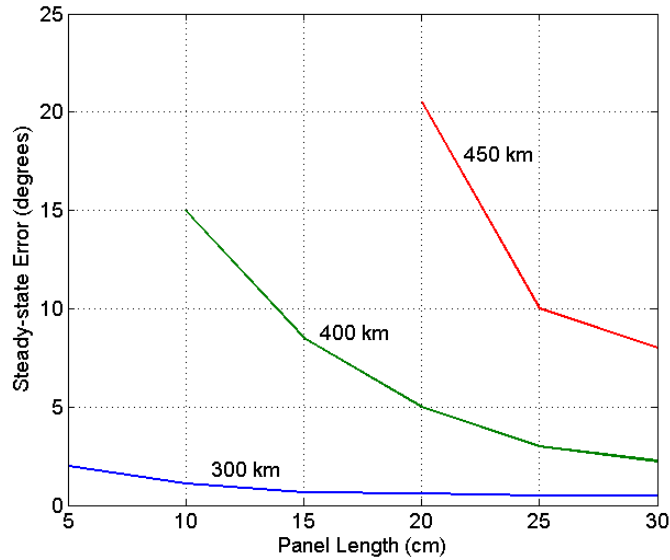


Figure 4-6: Effect of varying the Panel Length (λ) at different altitudes for panels deployed at $\theta = 50$ deg, computed using actual calculated torque profiles.

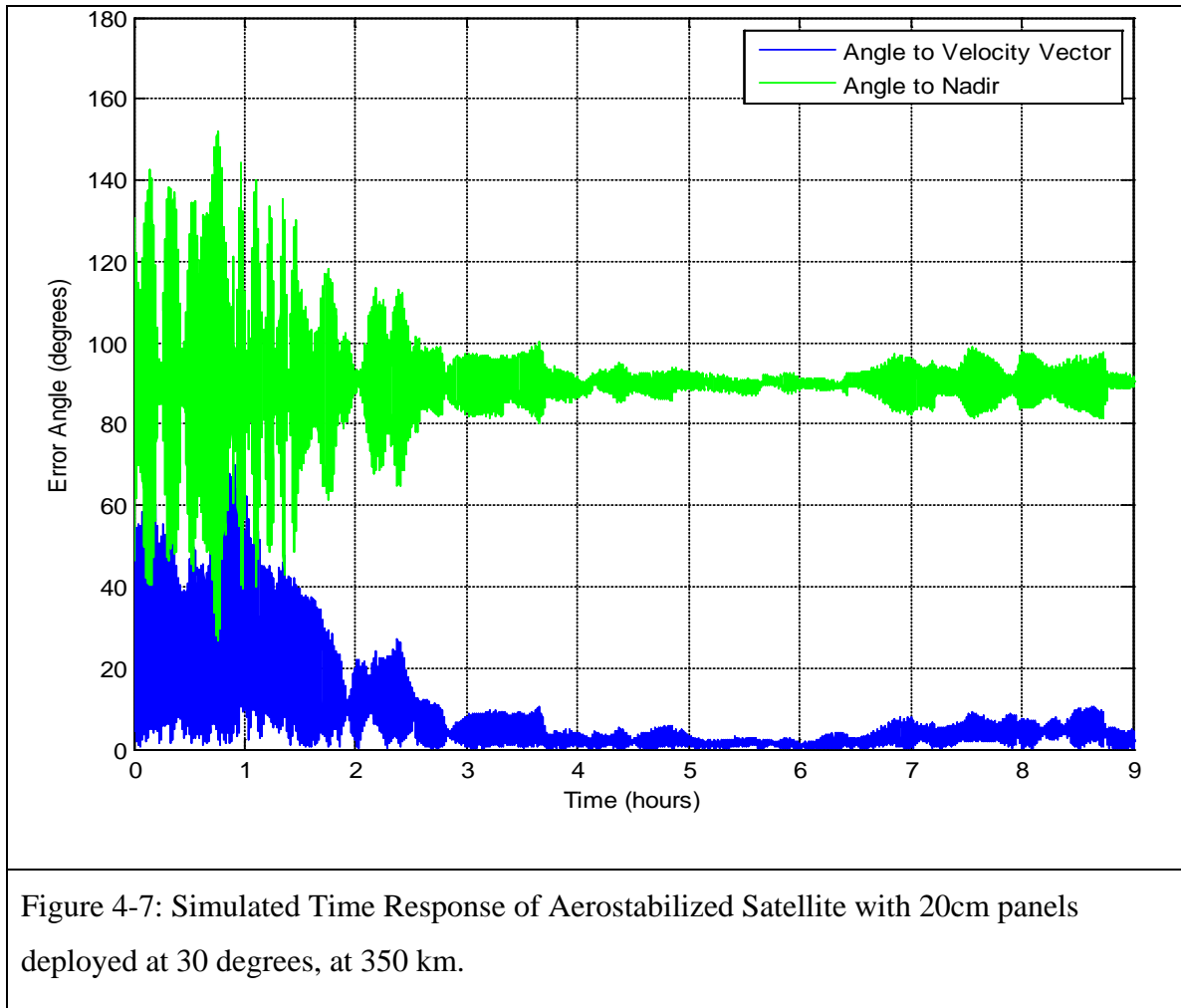
4.3 Simulation Results

This section presents the simulated response of an Aerostabilized Satellite. The selected configuration of 20 cm panels deployed at 30 degrees was simulated at 350 km. Table 4-1 summarizes the satellite design and simulation parameters.

Table 4-1: Aerostabilization Simulation Parameters

| Parameter | Details | Description |
|---------------------|------------------|----------------------------------------------------|
| Deployable Panels | Panel Length | 20 cm |
| | Panel Width | 10 cm |
| | Deployment Angle | 30 ° |
| Hysteresis Material | Type | HuMu80 |
| | Total Volume | 2.4 cm ³ (0.8 cm ³ per axis) |
| | Coercivity | 1.59 A/m |
| | Saturation | 0.73 Tesla |
| | Remanence | 0.35 Tesla |
| Orbit Parameters | Orbit Altitude | 350 km |
| | Inclination | 98° |

Figure 4-7 shows the time response of the simulation. The angle relative to the velocity vector is plotted in blue, and the angle relative to the nadir vector is in green. It appears that the satellite begins to track the velocity vector within 3 hours. The plot of the angle to nadir also shows the satellite lining up with the velocity vector 90 degrees from the nadir vector (for a circular orbit).

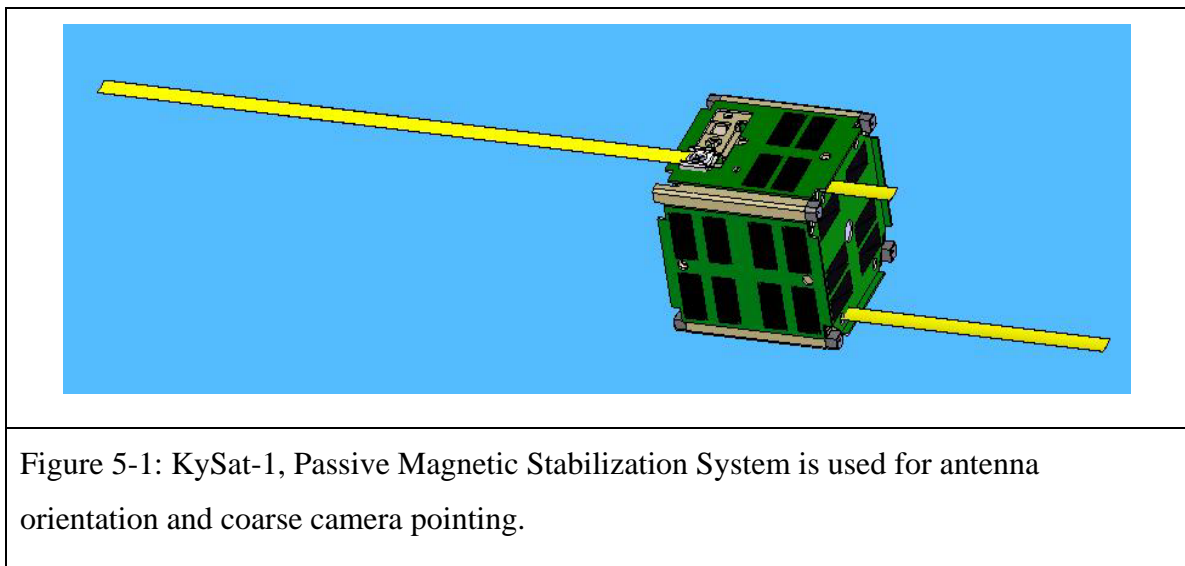


5 Passive Magnetic Stabilization

5.1 Introduction

This chapter describes the use of permanent magnets and magnetic hysteresis material to stabilize KySat-1, the first CubeSat developed by Kentucky Space. KySat-1 is expected to be launched into a polar sun-synchronous orbit having an altitude of about *708 km* and an inclination of 98° . The passive stabilization system is included to orient the main VHF/UHF radio antennas' main lobes towards Kentucky.

KySat-1 uses a set of Alinco-5 permanent magnets mounted in the corners along the z-axis of a Pumpkin CubeSat[15]. The goal is to orient the Antennas' main lobes and camera payload. Figure 5-1 is a model of KySat-1, the magnets are located at the inside corners of the rails, parallel to the antennas. In the polar orbit with the permanent magnet stability system, KySat-1 should perform two rotations per orbit, tumbling over the north and south magnetic poles, and align the antennas with the ground at low latitudes. The amount of magnets that can be included is under the severe mass and volume constraints of a 1-U CubeSat.



Sections 3.2.2 and 3.2.3 describe the physical phenomena and the mathematical modeling

of magnetic torque and hysteresis material. The remainder of this chapter describes the design and simulation results of the passive magnetic stabilization system of KySat-1.

5.2 Design

5.2.1 Magnets

The strength of the magnets should be chosen to be strong enough to overcome the greatest expected disturbances. Table 5-1 lists the calculated worst-case expected disturbance torques at an altitude of *700 km*. In the calculations, the satellite has a center of mass *2 cm* from the geometric center, which is the worst allowable according to the current CubeSat standard. A residual magnetic dipole of 0.01 A.m^2 in the spacecraft structure is assumed in the table. [reference RMIT]

| Torque Source | Amount | Units |
|--------------------------|------------|-------|
| Aerodynamic | 8.7175E-10 | N.m |
| Gravity Gradient | 6.8057E-10 | N.m |
| Solar Pressure | 3.7724E-09 | N.m |
| Residual Magnetic Moment | 4.5303E-07 | N.m |
| TOTAL | 4.5835E-07 | N.m |

Table 5-1: Worst-case expected disturbance torques for a 1-U CubeSat at 700 km.

Due to the stacked configuration and volume restrictions inside the structure of KySat-1, the largest possible permanent magnetss were included in the four inside corner rails. Figure 5-2 is a sketch of the location and polarity of the permanent magnets. The total resulting magnetic dipole strength was comparable to other CubeSats. The design of the magnetic hysteresis material amount and simulations to evaluate the performance followed that design choice.

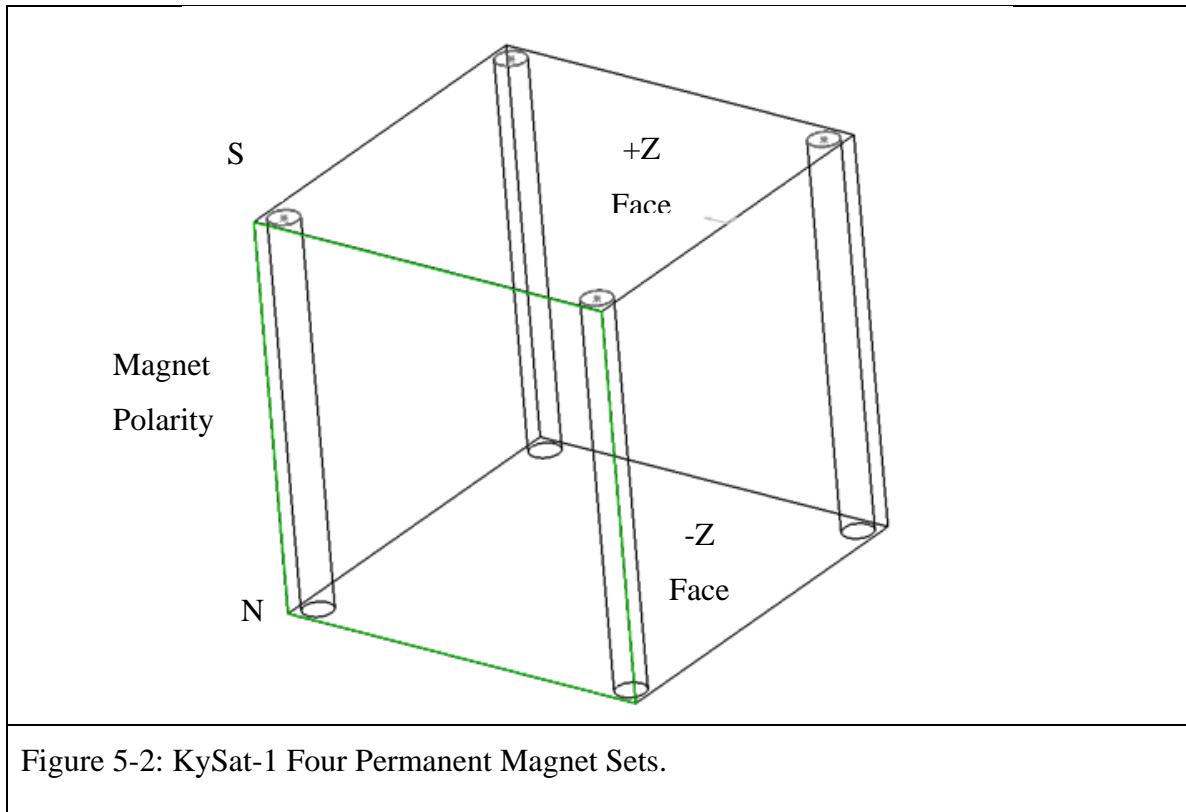


Figure 5-3 is a photograph of one of the inner corners of the KySat-1 frame. Each corner has 6 magnets each with a 0.15 cm diameter, and a length of 1.27 cm. The total number in all four corners is 24 magnets. The total magnetic dipole of all 24 magnets is calculated to be 0.5869 Am^2 . Table 5-2 summarizes the details on the KySat-1 passive magnetic stabilization system.

Table 5-2: KySat-1 Passive Magnetic Stabilization System Summary

| Item | Description |
|-----------------------|----------------------------------------------------------------|
| Magnet Material | Alinco-5 |
| Total Volume | 0.59 cm^3 |
| Total Magnetic Dipole | 0.5869 Am^2 (calculated) |
| North Pole | CubeSat -Z face |
| Hysteresis Material | 0.15 cm^3 distributed on CubeSat +Z face solar board |



Figure 5-3: One of Four Alinco-5 Permanent Magnet sets on board KySat-1.

5.2.2 Hysteresis Damping

A form of angular rate damping must accompany the permanent magnets. Magnetic hysteresis material is a completely passive solution that is commonly used in Small Satellites. Active damping using magnetic coils is also possible, such a design is described in [7]. For KySat-1, a passive solution utilizing a certain amount of HyMu80 sheet material was used.

Simulations show that none or too little hysteresis material does not stabilize a satellite, oscillations are too great and energy induced into the system from the magnets and perturbations is not dissipated and the satellite exhibits a twisting tumble. Increasing hysteresis material beyond the suitable amount was observed to increase the tracking lag between the magnet axis and the earth's magnetic field lines. Simulations with excess hysteresis material had the satellite lagging the magnetic field lines to the extent of not tracking the magnetic field lines. It was also noticed that the optimal amount of hysteresis

is directly proportional to the permanent magnets' strength.

The above guidelines impose the upper and lower limit on the amount of hysteresis material to include. There are however other unpredictable considerations that affect the design choice:

- The oscillation frequency about the magnetic field lines increases the stronger the magnets are.
- The greater the amount of hysteresis material, the greater the steady-state error (lag) relative to the magnetic field lines.
- The hysteresis material may suffer from saturation from the permanent magnets included in the satellite, since hysteresis material is not truly anisotropic (directional). A bias in the hysteresis material would make the earth's magnetic field sweep smaller areas and reduce heat loss. The performance of a certain amount of hysteresis material would be overestimated under this phenomenon. This motivates including a larger amount of hysteresis material.
- Other components in the spacecraft, such as the structure for example, contribute to damping with hysteresis and Eddie Current effects to a small degree. The hysteresis effects the satellite undergoes would be under-estimated when simulated for a certain amount that is assumed to be solely due to hysteresis material. This motivates a conservative design.
- Satellite material surrounding the hysteresis material could shield the magnetic field, and make it less effective. This factor motivates including more hysteresis material.

Figure 5-4 shows two design plots that were used to select an appropriate amount of hysteresis material. Simulations were run with fixed initial tumble conditions and variable hysteresis material amounts. The detumbling time to finally track the magnetic field was recorded for a range of hysteresis material amounts. The error angle (lag) in tracking the magnetic field was also recorded. The first plot which highlights the tracking error as a function of the amount of hysteresis material, implies the smallest possible

amount of hysteresis material should be selected to minimize the tracking error; the greater amount of hysteresis material the greater the lag and error. The second plot which shows the detumbling time as a function of hysteresis material volume on board KySat, exhibits a curve that motivates to design for the maximum possible amount of hysteresis to minimize detumbling time. This curve is used as a measure of how effective the hysteresis material is at damping oscillations and dissipating energy. The plot shows that too little hysteresis would result in a very long detumbling time, approaching instability. Given the uncertainty in effectiveness of a certain amount of hysteresis material, the knee of the curve is selected to minimize the sensitivity to any estimation errors. A volume 0.075 cm^3 of HyMu80 material per axis gives a detumbling time of 580 minutes from a 0.5 rad/s initial tumble, and a tracking lag of 9° relative to the magnetic field local to the satellite.

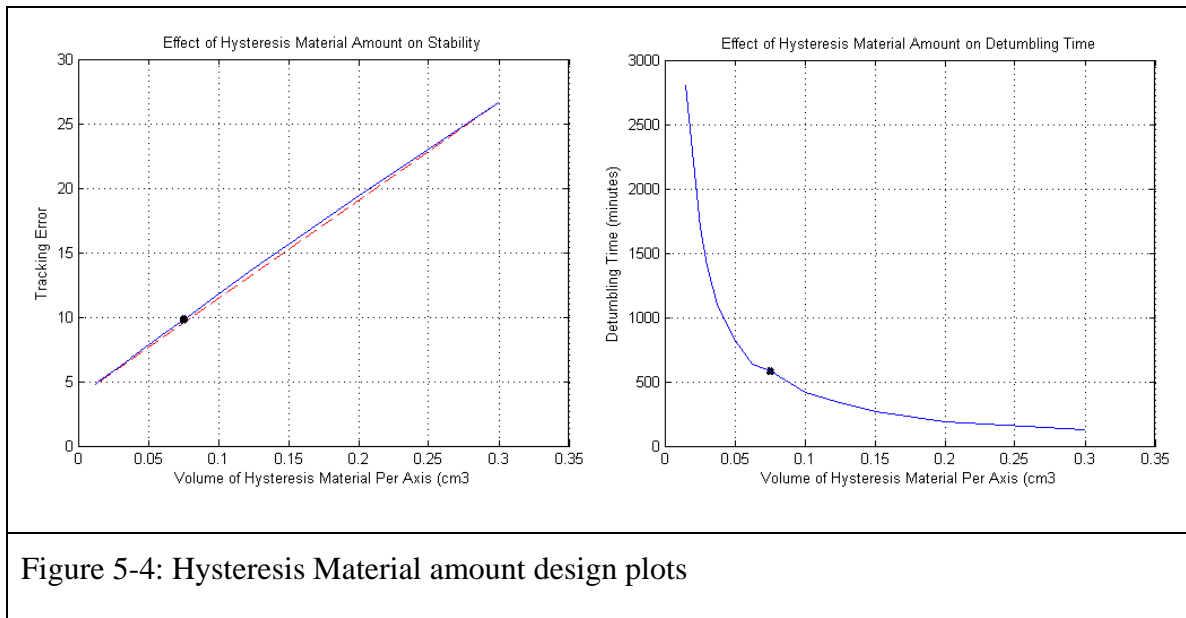


Figure 5-5 shows the back of the bottom solar board with the hysteresis material mounted to it. Using a magnetometer, it was found that the magnetic field from the permanent magnets is smallest at that point.

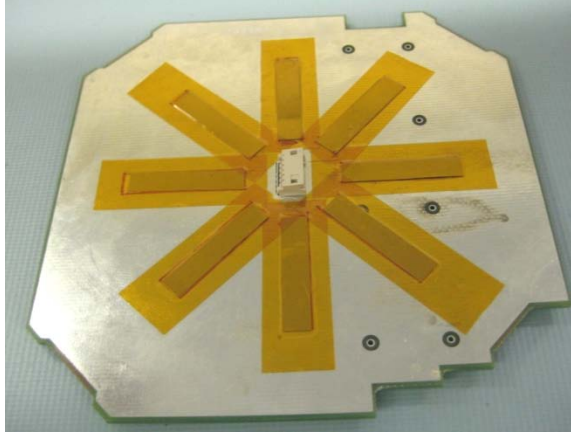


Figure 5-5: Hysteresis strips on the back of a solar board, on KySat-1

5.3 System Performance

This section shows the simulation results of KySat-1 in the Attitude Propagator that is developed in this thesis. Table 5-3 lists the simulation parameters. The satellite is placed in a sun synchronous orbit at 708 km, at an inclination of 98° .

Table 5-3: KySat-1 Passive Magnetic Stabilization System Simulation Parameters

| Parameter | Details | Description |
|---------------------|-----------------------|------------------------------------------------------|
| Magnets | Magnet Material | Alinco-5 |
| | Total Volume | 0.59 cm^3 |
| | Total Magnetic Dipole | 0.5869 Am^2 (calculated) |
| | North Pole | CubeSat -Z face |
| Hysteresis Material | Type | HuMu80 |
| | Total Volume | 0.15 cm^3 (0.075 cm^3 per axis) |
| | Coercivity | 1.59 A/m |
| | Saturation | 0.73 Tesla |
| | Remanence | 0.35 Tesla |
| Orbit Parameters | Orbit Altitude | 700 km |
| | Inclination | 98° |

Figure 5-1 shows the time response of the simulation. The angle relative to the magnetic field local to the satellite is plotted in blue, and the angle relative to the nadir vector is in green. It appears that the satellite begins to track the magnetic field within 1.5 hours. The plot of the angle to nadir shows the satellite tumbling over itself about once every 90 minutes (once per orbit).

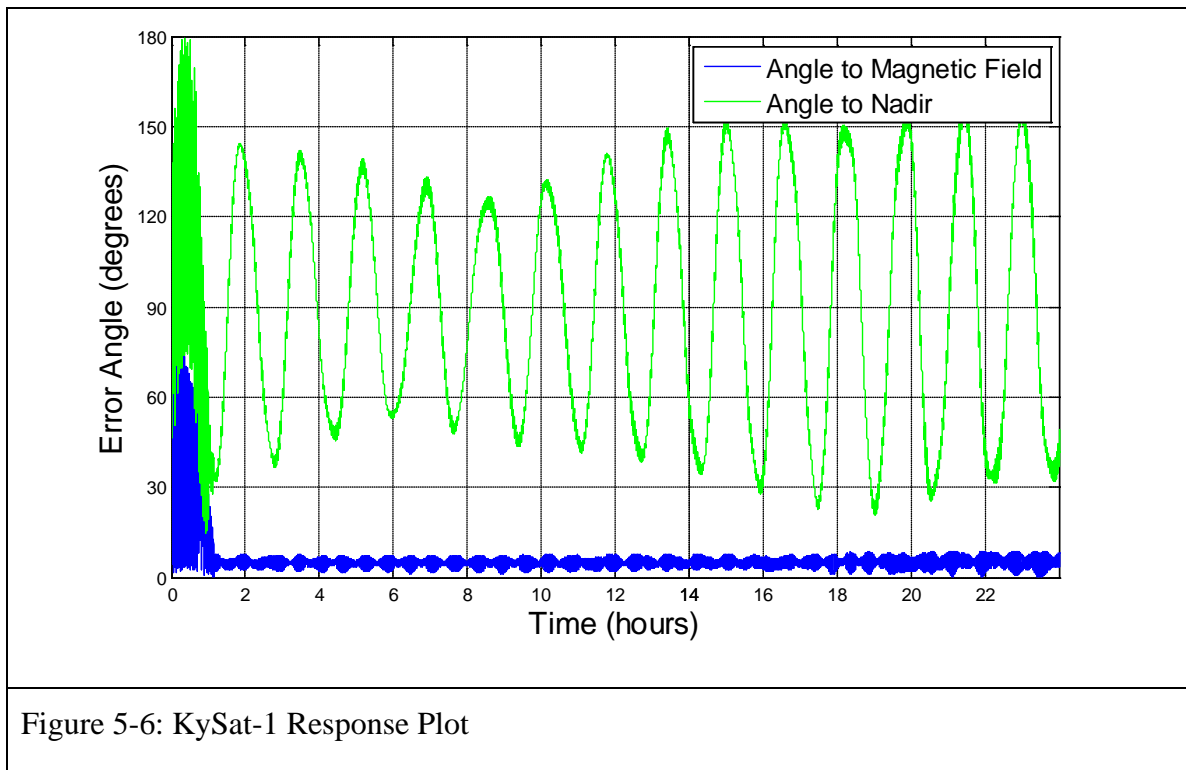


Figure 5-6: KySat-1 Response Plot

6 Conclusions

The Orbital Environment Simulator was developed to study various attitude stabilization systems. The major environmental torques from a small-satellite perspective (gravity gradient, magnetic, and aerodynamic) were modeled in Simulink, as well as magnetic hysteresis material which is a passive solution to angular rate damping. The model basically reads in the satellite description and design parameters, and propagates it throughout its orbit. At each time step, the various environmental torques are calculated given the magnetic field at that point, the velocity, position in orbit, and the satellite orientation. The satellite position and orientation are modeled by a 6-DOF body model. Simulink offers a variety of differential equation solvers to propagate the models and obtain attitude reports for analysis and animation.

Passive magnetic stabilization is very attractive and often used for small satellites that are light enough to gain basic pointing or to merely avoid random and unpredictable tumble. Using permanent magnets to gain stability is a proven concept that is implemented on several CubeSats currently in orbit. The choice of the magnet strength and amount of hysteresis damping material is dependent on the geomagnetic field and disturbance torques at the orbit under consideration. Simulation and attitude propagation is a very convenient tool to experiment with different designs and to study the dynamic response.

Achieving aerodynamic stabilization passively using magnetic hysteresis for damping was more challenging compared to magnetic stabilization. The dynamic response was sensitive to the amount of hysteresis material; small variations caused great changes in steady-state behavior and often instability. Also, since the atmospheric density varies exponentially with altitude, the same satellite design would behave differently as a function of altitude. Compared to gravity gradient stabilization and passive magnetic stabilization that are fairly simply described in the mass properties and the magnet content, aerodynamic stability has a much larger design space because it depends on the outer geometry. Research and experimentation in spacecraft aerodynamics and active

surface articulation in lower orbits appears to be of interest within the small-satellite community and may have future prospects.

Gravity gradient stabilization is perhaps the simplest of the three stabilization techniques discussed in this thesis. Gravity gradient torque is one of the predominant environmental effects for asymmetric satellites and acts as the major disturbance torque for the other stabilization systems. Using a gravity gradient bias in the mass distribution of the satellite to overcome the other environmental torques is easily achieved; the stable design space is relatively large compared to the other stabilization problems. Angular rate damping is however still an issue, and magnetic hysteresis damping material is again a passive solution and can be chosen by running a set of simulation.

The Orbital Environment Simulator is also a platform for future work on active attitude control systems, such as reaction wheels and active magnetic torque coil systems. A control system would be designed to maintain desired stability in the presence of the environmental torques which would act as the noise and disturbance in the system.

7 References

- [1] G. D. Chandler, D. T. McClure, S. F. Hishmeh, J. E. Lumpp, Jr., J. B. Carter, B. K. Malphrus, D. M. Erb, W. C. Hutchison, III, G. R. Strickler, J. W. Cutler, R. J. Twiggs., "Development of an Off-the-Shelf Bus for Small Satellites." Big Sky, Montana : s.n., 2007. IEEE Aerospace Conference.
- [2] Vallado, David A., *Fundamentals of Astrodynamics and Applications*. 3rd Edition. : Microcosm Press, 2007.
- [3] Wertz, James R., *Spacecraft Attitude Determination and Control*. : Microcosm Press, 1978.
- [4] Wie, Bong., *Space Vehicle Dynamics and Control*. : AIAA, 1998.
- [5] College of Engineering, Cornell University., *Ionospheric sCintillation Experiment CUBESat Project*. [Online] <http://www.mae.cornell.edu/cubesat/>.
- [6] Michael., *Michael's List of Cubesat Satellite Missions*. [Online] July 2009. <http://mtech.dk/thomsen/space/cubesat.php>.
- [7] Psiaki, M. L., "Nanosatellite Attitude Stabilization Using Passive Aerodynamics and Active Magnetic Torquing." *Journal of Guidance, Control, and Dynamicss*, 2004, Issue 3, Vol. 27, pp. 347–355.
- [8] B. M. Menges, C. A. Guadamos, E. K. Lewis., "Dynamic Modeling of Micro-Satellite Spatnik's Attitude." 1998. 36th AIAA Aerospace Sciences Meeting and Exhibit
- [9] Levesque, J., "Passive Magnetic Attitude Stabilization using Hysteresis Materials." 2003. 17th AIAA/USU Conference on Small Satellites.
- [10] MathWorks., *Choosing a Solver*. [Simulink Documentation] 2007.
- [11] F. J. Regan, S. M. Anandkrishnan., *Dynamics of Atmospheric Re-entry*. 1993.
- [12] Wiley J. Larson, James R. Wertz., *Space Mission Analysis and Design*. Third Edition. s.l. : Microcosm Press, 1999.
- [13] Sidi, Marcel J., *Spacecraft Dynamics and Control*. : Cambridge University Press, 1997.
- [14] S. Rawashdeh, D. Jones, D. Erb, A. Karam, and J. E. Lumpp, Jr., "Aerodynamic Attitude Stabilization for a Ram-Facing CubeSat." Breckenridge, Colorado : AAS 32nd Annual Guidance and Control Conference, 2009.

- [15] Pumpkin Inc., *CubeSat Kit*. [Online] <http://www.cubesatkit.com>.
- [16] H. Heidt, J. Puig-Suari, A.S. Moore, S. Nakasuka, R.J. Heidt., "CubeSat: A new Generation of Picosatellite for Education and Industry Low-Cost Space Experimentation." 2000. 14th Annual/USU Conference on Small Satellites.
- [17] R. R. Kumar, D. D. Mazanek, M. L. Heck., "Simulation and Shuttle Hitchhiker Validation of Passive Satellite Aerostabilization" . Vol. 32, No. 5, 1995, pp. 806–811." *Journal of Spacecraft and Rockets*, 1995, Issue 5, Vol. 32, pp. 806-811.
- [18] R. R. Kumar, D. D. Mazanek, M. L. Heck., "Parametric and Classical Resonance in Passive Satellite Aerostabilization." *Journal of Spacecraft and Rockets*, 1996, Issue 2, Vol. 33, pp. 228–234.
- [19] Bird, G. A., *Molecular Gas Dynamics*. : Oxford Univ. Press, 1976.
- [20] NASA., NASA Orbital Debris Program Office. [Online] <http://orbitaldebris.jsc.nasa.gov>.
- [21] S. Rawashdeh, D. Jones, D. Erb, A. Karam, and J. E. Lumpp, Jr., "Aerodynamic Attitude Stabilization for a Ram-Facing CubeSat." Breckenridge, Colorado : AAS 32nd Annual Guidance and Control Conference, 2009.
- [22] Wie, Bong., *Space Vehicle Dynamics and Control*. : AIAA, 1998.
- [23] MathWorks, The., *Simulink Aerospace Blockset Documentation*. : The MathWorks, 2009.
- [24] Sidi, Marcel., *Spacecraft Dynamics and Control*. : Cambridge University Press, 1997.
- [25] James R. Wertz, Wiley J. Larson., *Space Mission Analysis and Design*. : Microcosm, Inc, 1999.
- [26] Vallado, David., *Fundamentals of Astrodynamics and Applications*. : Microcosm, Inc, 2007.
- [27] Wertz, James R., *Spacecraft Attitude Determination and Control*. : D. Reidel Publishing Company, 1978.
- [28] Levesque, J., "Passive Magnetic Attitude Stabilization using Hysteresis Materials." : 17th AIAA/USU Conference on Small Satellites, 2003.

Vita

Personal

Citizenship: Jordan and Finland
Birth Place: Jeddah, Saudi Arabia
Date of Birth: June 11, 1984

Education

Bachelor of Science in Electrical Engineering, June 2007
Department of Electrical Engineering
University of Jordan, Amman, Jordan

Work Experience

Research Assistant

01/2008 - Current

Space Systems Laboratory, University of Kentucky, Lexington, KY

Full-time Research Assistant

06/01/2007 – 07/30/2007

Mechatronics Engineering Laboratory, University of Jordan, Amman, Jordan

Exchange Student Research Training

06/2005 – 08/2005

IDEA Laboratory, University of Kentucky, Lexington, KY

Publications

- S. Rawashdeh, D. Jones, D. Erb, A. Karam, J. Lumpp, “*Aerodynamic Attitude Stabilization for a Ram-Facing Cubesat*”, AAS Guidance and Control Conference 2009, Breckenridge, CO.
- S. Rawashdeh, J. Lumpp, “*Nano-Satellite Passive Attitude Stabilization Systems’ Design by Orbital Environment Modeling and Simulation*”, AIAA Infotech@Aerospace 2010, Atlanta, GA .
- J. Lumpp et. al., “*SOCEM: Sub-Orbital CubeSat Experimental Mission*”, 2010 IEEE Aerospace Conference, MT.